UNIVERSITÀ DI PISA

Facoltà di Farmacia

Corso di Laurea in

Chimica e Tecnologia Farmaceutiche

"Synthesis and biological evaluation of novel N,N-dialkyl-2-arylindol-3-ylglyoxylamide TSPO ligands„

Relatori:

Dott.ssa Sabrina Taliani

Prof.ssa Claudia Martini

Candidata:

Fanelli Serena

Anno accademico 2011/2012

Ad maiora!

ABSTRACT:

The 18kDa Translocator protein (TSPO) was discovered in 1977 and initially named "*Peripheral-type benzodiazepine receptor*" (PBR). It is located at the point of contact between inner and outer mitochondrial membrane. It is associated with other membrane proteins to form the mitochondrial permeability transition pore (MPTP). The expression of TSPO is ubiquitary in peripheral tissues (steroid producing tissues, liver, heart, kidney, lung, immune system), and in the central nervous system is mainly located in glial cells and in neurons. It is involved in numerous functions including steroidogenesis, the transport and the synthesis of heme, immunomodulation, the regulation of apoptosis and generation of radical oxigen species (ROS). In the 1995 Dalpiaz et al. proposed a pharmacophore model later refined by Da Settimo et al. in 2008. On the basis of these studies a series of *N*,*N*-dialkyl-2-phenylindol-3-ylglyoxylamide derivatives was synthesized and tested as TSPO ligands. The SARs of these compounds were rationalized in light of the pharmacophore/topological model of TSPO binding site made up of three lipophilic pockets (L1, L3 and L4) and a H-bond donor group (H1). The aim of this work is the design and the synthesis of a novel series of *N*,*N*-dialkyl-2-phenylindol-3-ylglyoxylamide featuring suitable substituentes on the indole nucleus for good pharmacokinetic parameters. The affinity towards TSPO of all the new compounds was tested by binding assays performed on rat kidney membranes. For those compounds which showed a K_i value in the sub-nanomolar range, the ability to induce functional effects trough the TSPO was also tested. In particular, since TSPO-related apoptosis and steroidogenesis are events which play key roles in the homeostasis of cellular processes, we carried out experiments on cell growth in metabolic stress conditions. The status of cellular stress was created by nutrient deprivation using low serum medium culturing conditions (1% fetal bovine serum FBS). The effects of some compounds (the most promising ones in term of affinity) were evaluated by proliferation MTS assay and crystal violet staining. The obtained results showed an increase in cell growth after 48 hours of treatment with compounds, in respect to the control. If such preliminary results are confirmed even in a cellular model of primary neurons or in a neurodegenerative cell model, these compounds may be used as versatile scaffold for the design of novel neuroprotective agents.

TABLE OF CONTENTS

INTRODUCTION:

The first benzodiazepine, chlordiazepoxide (Librium), was discovered accidentally in 1955 by Leo Sternbach, and made available in 1960 by Hoffmann-La Roche, who also marketed as diazepam (Valium) since 1963.[1] Starting in the sixties and seventies benzodiazepines have begun to be widely prescribed clinically. The extensive clinical use is based on their activities of powerful anxiolytics, anticonvulsants, sedative-hypnotics and muscle relaxants.[2] In humans exist two different forms of benzodiazepine receptors: central benzodiazepine receptors (***CBRs***) and peripheral benzodiazepine receptors (***PBRs***).

The first type (CBRs) is found in the brain and forms an allosteric site on the $GABA_A$ receptor complex. In fact, ligands acting at this allosteric site, such as diazepam and chlordiazepoxide, enhance the affinity of the γ-aminobutyric acid (***GABA***) toward the CBR and, in this way, influence chloride (Cl^-) influx at the $GABA_A$ receptor pore, causing downstream effects on GABA-mediated inhibition.[3] Different studies have shown benzodiazepines (***BZs***) acting on CBRs to be responsible for different $GABA_A$-induced effects.

The second type (PBRs) is first described in 1977 by Braestrup and Squires[4] as an alternative binding site in non-neuronal tissue for the diazepam, a centrally acting benzodiazepine. It was named peripheral according to this tissue distribution and benzodiazepine receptor because BZs is the class of ligands by which PBR was discovered. However, multiple other names have been used to refer to this protein, including mitochondrial benzodiazepine receptor (MBR), mitochondrial diazepam

binding inhibitor (***DBI***) receptor complex (***mDRC***), PK11195 binding sites (***PKBs***), isoquinoline binding protein (***IBP***), Omega3 receptor. [5]

Recent data have increasingly supported the renaming of this protein with the aim to represent more accurately its sub-cellular role and putative tissue-specific functions. In 2006, a team of scientists has proposed the new name Translocator Protein (18 kDa), TSPO. [6] In fact the name PBR was widely accepted mainly for historical reasons in the scientific community, but it didn't take into account the new findings regarding its structure, subcellular roles and tissue distribution. It has also been shown that many ligands structurally different from BZs bind to this protein, which is not a receptor in the traditional sense, but rather a translocator of molecules. TSPO is an evolutionarily well-conserved and tryptophan rich 169-amino acids protein with five trans-membrane domains which consist of extended α-helices composed of 21 residues, long enough to spam an entire membrane bilayer. These α-helices are linked by hydrophobic loops, with a carboxyterminal and a short amino-terminal tails located outside and inside the mitochondria, respectively. Furthermore, site-directed mutagenesis studies demonstrated that the portion of the receptor that recognized the ligands is located on the first cytoplasmatic loop TSPO forms complexes of four to six molecules whose organization is postulated to form a single pore, reflecting the function of TSPO as a transporter protein in the mitochondrial membrane. [5] The TSPO active shape appears the dimeric.[7]

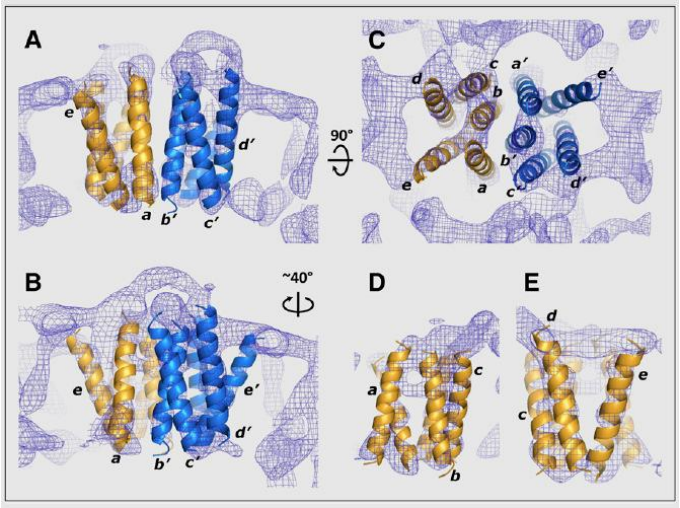

FIGURE (1): *Three-dimensional structure of TSPO. (A) View perpendicular to the plane of the membrane of the TSPO dimer. (B) View parallel to the plane and after rotation of 40 °. (C) View perpendicular to the plane after 90 ° rotation. (D) Monomer TSPO view parallel to the plane from the side of the interface with the dimer. (E) TSPO monomer seen from the lipid bilayer.*

However, the exact three-dimensional structure of TSPO has not yet been determined, as its close association to the membrane makes the purification and crystallization processes very difficult to accomplish. At a subcellular level, TSPO is mainly located on the mitochondrial outer membrane and particularly concentrated at outer/inner mitochondrial membrane contact sites. In addition, TSPO is also expressed at low levels in other subcellular compartments, such as plasma membranes and nuclear fraction of cells. In 1992 McEnery et al. reported that TSPO is strictly associated in a trimeric complex with ***VDAC,*** a voltage-dependent anion channel of 32 kDa located at sites of contact between outer and inner mitochondrial membrane that acting as a channel allowing passage of small molecules and ions into the mitochondria, and ***ANT***, adenine nucleotide translocase, a specific antiporter of 30 kDa, located in the inner mitochondrial membrane, for the exchange of ATP and ADP as part of oxidative

phosphorylation. Together with other proteins, these three sub-units constitute the mitochondrial permeability transition pore (***MPTP***).[8]

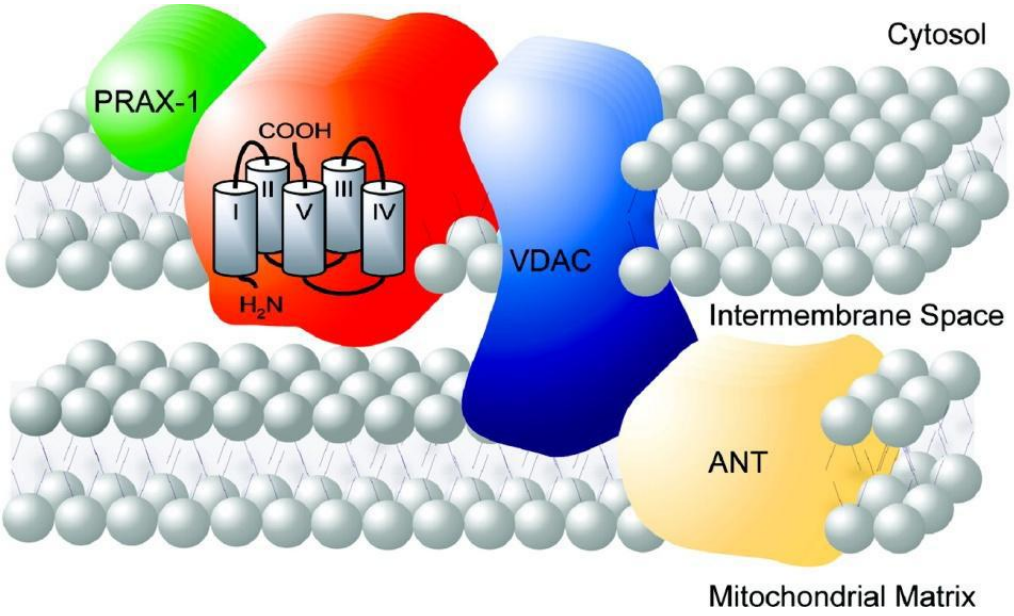

FIGURE (2): *Molecular structure of 18kDa TSPO and localization. It is also shown some proteins as-sociated with TSPO in the MPTP complex (VDAC, ANT and PRAX-1)*[8]

Furthermore, it has been identified four cytosolic TSPO-associated proteins which most of time play an important role in the biological processes where TSPO is involved. ***p10*** is the first cytosolic protein associated to TSPO identified, but whose bio-chemical role has not been understood yet. It is a protein of 10 kDa that coimmunoprecipited with 18 kDa TSPO using the isoquinoline carboxamide radioactive probe ***PK14105***, a ligand selective for mitochondrial benzodiazepine receptors, to photolabel rat mitochondrial preparations.[9]

PBR associated protein-1 (***PRAX-1***) is isolated, cloning and characterized by Galiègue et al. in 1999.[10] It is a protein of 1857 amino acids with a molecular mass of 240 kDa, discovered using the yeast two-hybrid screening strategy. Exhibiting various domains involved in protein-protein interaction, such as proline-rich domains, leucine-zipper motifs and Src homology region 3-like (***SH3***-like) do-

domains, it has been suggested that PRAX-1 acts as an adaptor protein to recruit additional targets to the vicinity of TSPO so as to modulate its function. In addition, it was assumed that a single PRAX-1 protein interacts with the C-terminal end (14 amino acids) of several molecules of TSPO (at least two of them).

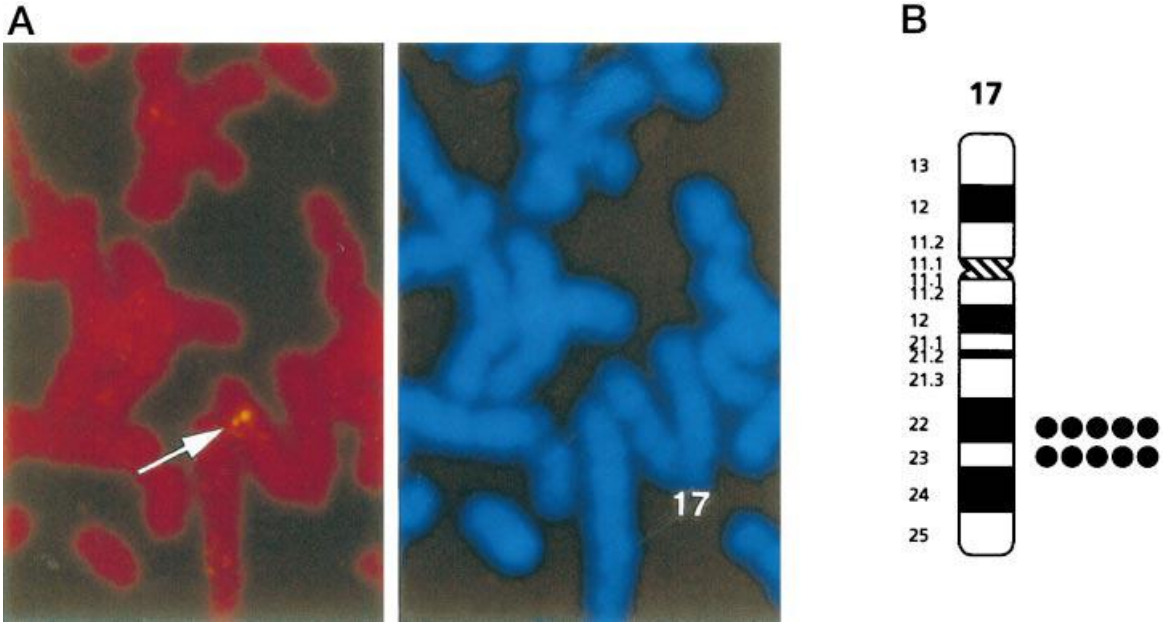

FIGURE (3): *Chromosomal localization of the human PRAX-1 gene. A, FISH mapping of the human PRAX gene. The left panel shows the FISH signals on chromosome. The arrow indicates the specific site of hybridization to chromosome 17. The right panel shows the same mitotic figure stained with DAPI to identify chromosome 17. B, idiogram of the human chromosome 17 illustrating the distribution of labeled sites for the human PRAX-1 probe. Each dot represents the double FISH signals detected on human chromosome17.*

Another important protein functional associated to TSPO is Steroidogenic Acute Regulatory Protein (***StAR***), that mediates the flow of cholesterol from the outer to the inner mitochondrial membrane, permitting steroid formation in steroidogenic cells. Further studies indicated that StAR acts at the outer mitochondrial membrane and it is not needed to allow the entry of cholesterol into mitochondria. Therefore, Hauet et al. suggest that TSPO and StAR work in concert to bring cholesterol into mitochondria and in particular TSPO serves as a gatekeeper in cholesterol import into mitochondria and StAR plays the role of the hormone-induced activator.[11, 12]

FIGURE (4): *Biological Assembly Image for 3P0L. Human steroidogenic acute regulatory protein.*

PKA-associated protein 7 (***PAP7***) is a cytosolic protein with a molecular mass of 52 kDa involved in the hormonal regulation of steroid formation, interacting with both the cytosolic RI_{α} subunit of PKA and TSPO. Particularly, PAP7 targets the PKA isoenzyme, linked to increased steroid synthesis, which phosphorylating specific protein substrates induces the reorganization of TSPO topography and function.[13]

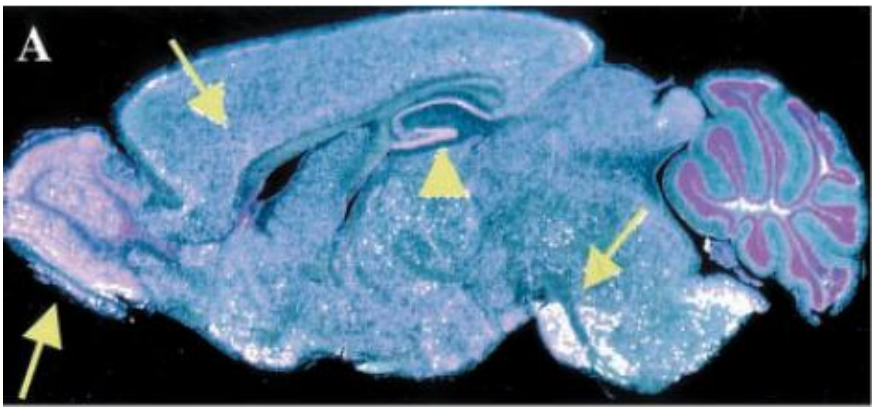

FIGURE (5): *mRNA Expression of PAP7 in Mouse Tissues Examined by in Situ Hybridization with an antisense 35S-labeled cRNA probe to full-length PAP7. Brain sagittal section.*

ROLE OF TSPO IN CELLULAR FUNCTION:

✓ *REGULATION OF STEROIDOGENESIS.*

The location of TSPO on the outer mitochondrial membrane and the extremely high density in steroidogenic endocrine tissues, such as adrenocortical cells and Leydig cells, suggest that TSPO plays an important role in steroidogenesis. Moreover, different publications report that this protein ligands stimulate steroid biosynthesis in adrenal, placental, testicular, ovarian and glial systems.[14, 15]

The biosynthesis of steroids begins with the enzymatic transformation of cholesterol into pregnenolone, which occurs through cholesterol side-chain cleavage by the cytochrome P450scc (***CYP11A1***) and auxiliary electron transferring proteins, localized on the matrix side of the inner mitochondrial membrane. Pregnenolone then leaves mitochondria to move to the endoplasmic reticulum, where it is transformed in the final steroid products. [6, 7, 11]

The rate-limiting step is the translocation of cholesterol from the cellular stores across the aqueous intermembrane space to the inner mitochondrial membrane and P-450scc. The fundamental role of TSPO in this mitochondrial cholesterol transport and thus in steroids synthesis is supported by numerous data, and particularly knockout and antisense experiments in vitro have demonstrated that down-regulation of TSPO causes a decrease in steroid synthesis.[7, 14, 15]

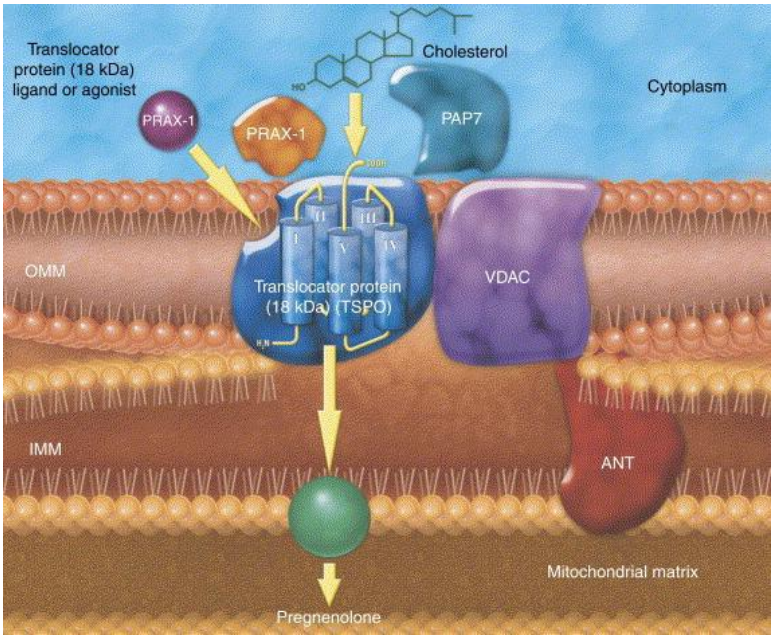

FIGURE (6): *Transport of cholestrerol, across the mitochondrial membrane, from the intracellular space within the mitochondria, by the TSPO.*

The topographic study of TSPO in the mitochondrial membranes have also shown that after treatment of Leydig cells with a steroidogenesis stimulator, such as choriogonadotrophin hormone (***hCG***), there are various morphological changes, such as a formation of large complexes of 15-25 molecules of TSPO and a rapid reorganization of their localization in the mitochondrial membrane, as well as a rapid increase in TSPO ligand binding.[7, 14]

Moreover, amino acids deletion, site-directed mutagenesis and structural studies have permitted to identified a cholesterol recognition amino acid consensus (***CRAC***) sequence in the cytosolic carboxy-terminal domain of the TSPO that could be part of the binding site for the uptake and translocation of cholesterol (channel-like interaction) through a channel delimited by five α-helixes of TSPO. However, for cholesterol delivery into mitochondria TSPO-mediated is also required the interaction of TSPO with StAR, a protein acting as hormone-induced activator.[6, 7,

[14] It has been observed a relationship between steroid levels, TSPO levels and anxiety, principally due to the fact that neurosteroids are endogenous modulators of the $GABA_A$ receptor. In general TSPO levels, determined by radioligand binding to platelets, decrease in patients with anxiety disorders. Therefore, ligands binding to TSPO located in glial cells, such as *N*,*N*-dialchyl-2- pheniylindol-3-ylglyoxylamides synthesized by Da Settimo et al.,[16] provide the cholesterol necessary to restore neurosteroid synthesis and increase pregnenolone formation, which is then metabolize to form allopregnanolone, a potent allosteric modulator of the $GABA_A$ exerting anxiolytic effects. In this sense TSPO could be considering a promising target for the psychiatric disorders that involve dysfunction in steroid biosynthesis.[11, 17]

It also has been observed that the systemic levels of steroids increase as a result of a lesion, to a pain or a fever, in response to stimulation by certain cytokines secretion of corticotropin releasing factor. The involvement of TSPO in the synthesis of steroids can contribute to this defense mechanism.[20]

- ✓ ***REGULATION OF APOPTOSIS***

MPTP plays an important role in the modulation of signaling pathways mediating apoptotic and necrotic cell death. The exact composition of the MPTP is not yet established, but it has been recognized various proteins implicated in pore formation and its regulation: an hexokinase, in the cytosol; a trimeric complex constituted by VDAC, ANC and TSPO; a creatine kinase in the intermembrane space and cyclophilin D in the matrix. MPTP allows the transfer of solutes, including ATP/ADP exchange, from the mitochondrial matrix to cytosol, through

the VDAC/ANC conduit, and there-fore facilitates the crossing of the highly impermeable mitochondrial inner membrane. This periodic transient increase in permeability by the MPTP allows the pumping of protons from the inner membrane by the electron transport chain and creates the transmembrane electrochemical gradient that derives ATP synthesis.[7, 18]

Several factors cause the opening of the MPTP: high [Ca^{2+}] is the fundamental trigger but alone is not enough, also low adenine nucleotide concentrations, high phosphate concentrations, oxidative stress and pro-apoptotic proteins. Pore opening leads to the dissipation of transmembrane electrochemical gradient, uncoupling of mitochondria and swelling, resulting in the release of cytochrome c and apoptosis inducing factor (***AIF***) into the cytosol. Once in the cytosol, the first induces the caspase cascade ending in the destruction of cell nucleus, cytoskeleton and plasma membrane; the second principally leads to nuclear chromatin condensation, DNA fragmentation and then to cell death.[18]

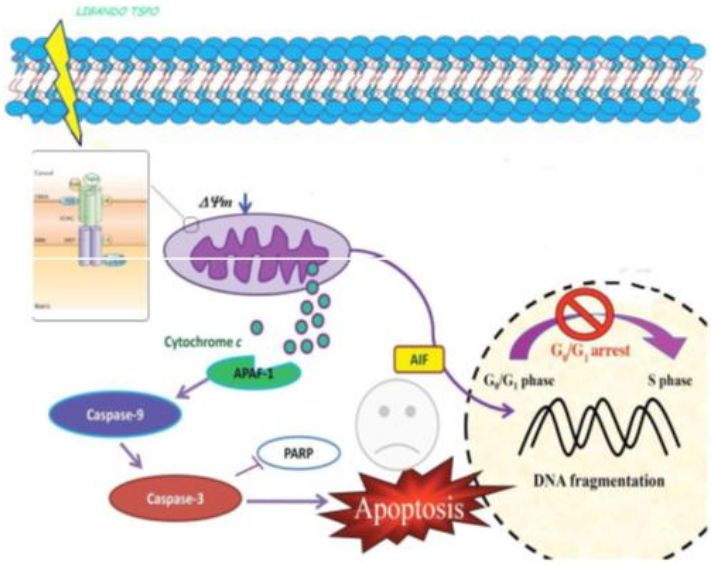

FIGURE (7): *Intracellular events which follow the MPTP opening and lead to apoptosis.*

The exact events which TSPO modulates apoptosis are still unknown. In 2008 Veenman et al.[34] suggested that interaction between VDAC and TSPO is fundamental to initiate the mitochondrial apoptosis pathway. The intermediary agent between TSPO and VDAC was supposed to be provided by mitochondrial ***ROS*** (reactive oxygen species) generation under the control of the same TSPO. ROS lead first to dissociation of cytochrome c from oxidized cardiolipins located at the inner mitochondrial membrane and, subsequently to its release in the cytosol via formation of a pore due to assemblage of VDAC molecules. In 2007 Azarashvili et al.[19] supposed another possible mechanism that provided evidence for TSPO involvement in MPTP opening, controlling the $Ca2^{+}$-induced $Ca2^{+}$ efflux and AIF release from mitochondria, important stage of initiation of programmed cell death. It has also been observed a modulation by TSPO of interactions between VDAC or ANT and pro-apoptotic or anti-apoptotic proteins (***Bcl-2*** and ***Bax***). Therefore, it has been designed TSPO ligands with pro-apoptotic effects acting as anticancer agents.[20]

- ✓ ***IMMUNOMODULATION***

The presence of the TSPO in a large number of cells immunomodulatory such as the microglia, the blood monocytes, lymphocytes, and leucocit, led to think of an involvement of TSPO in the immune response. It has been shown, in special studies in mice, that some TSPO ligands, specifically benzodiazepines, have an immunosuppressive action, inhibiting the capacity of macrophages to produce ROS and inflammatory cytokines such as ***IL-1*** (interleukin-1), $\boldsymbol{TNF_{\alpha}}$ (tumor necrosis factor alpha) and ***IL-6***, and regulating phagocyte oxidative metabolism required for

elimination of foreign antigens. Moreover, the TSPO is involved in oxidative metabolism by phagocytes, a process necessary to permanently delete the foreign antigens. The immunosuppressive action of certain ligands for the TSPO shown the important role played by this protein in the inflammatory response. [7]

✓ *TSPO AND NEUROINFLAMMATION*

The neuroinflammation are characteristic of many pathological conditions including neurodegenerative diseases such as Alzheimer, Parkinson's disease, metabolic and hepatic encephalopathy and repair processes following damage to cerebral and peripheral level.[21]

Specific ligands with nanomolar affinity for the TSPO, such as PK 11195 and Ro5-4864, were used to determine the parameters of the interaction ligand-receptor in brain tissue. The TSPO has been identified in the ependymal cells in the olfactory bulb and the choroid plexus later in glial cells, including microglia and astrocytes. Using the radioligand [^{3}H]-PK 11195 in animal models has been found an increase of the concentration of TSPO in numerous neurological diseases including multiple sclerosis, brain trauma, encephalitis and stroke. In most of these studies it was found an up-regulation of TSPO where the microglia is activated. Thanks to recent studies is possible obtain images of activated microglia through the use of PET(positron emission tomography) with ligands for the TSPO labeled with ^{11}C or ^{18}F.

✓ *OTHER FUNCTIONS*

Numerous studies on the functions of TSPO shown the modulation of its expression in physiological and pathological states, including the cellular response

in viral infections. One of the strategies adopted by viruses to bypass the protective mechanisms of cells against infection is to block apoptosis. Several pathogenic viruses using just the TSPO as a target to implement this block. This discovery therefore offers numerous prospects for new antiviral strategies.[20]

Other functions included protein import, important for membrane biogenesis and confirmed by the observation that TSPO is necessary for the import of StAR protein into mitochondria; TSPO, binding of dicarboxylic porphyrin and transport into mitochondria, have been reported as well as a relationship between TSPO and heme biosynthesis pathway; ion transport and calcium homeostasis, since it has been shown that TSPO regulates the Ca^{2+} flow into the cell. Furthermore, TSPO plays an important role in cellular respiration and mitochondrial oxidation, and affects cellular proliferation and differentiation in a number of cell types.[6]

The activity of TSPO is also implicated in stress. Its activation during acute exposure to stressors can be seen as a predisposition to metabolic and neuronal better adaptation to stress.[20]

High expression of this receptor has also been observed in neoplastic cells and tissues of the ovary, and adenocarcinom in the liver and colon cancer. This increase is correlated with the degree aggressiveness of tumor. The monitoring of the expression of this receptor, therefore, may be relevant in a clinical procedure for diagnosing and/or to follow the progression of the disease.

TSPO LIGANDS:

✓ TSPO ENDOGENOUS LIGANDS

A wide variety of endogenous molecules with affinity for the TSPO and different chemical structures have been identified. One of the first molecules identified, isolated both at central and pheripheral tissues (adrenal gland, kidney and testes), is a residue of neuropeptides (11 kDa) composed of 86 aa, which inhibits the binding of diazepam with the receptor site of the BZs called "inhibitor of the binding of diazepam (***DBI***)". In addition to this molecule and its metabolites have been isolated other endogenous ligands: Protoporphyrins (***protoporphyrins IX, mesoporphyrins IX, deuteroporphyrins IX, hemin***) exhibit a very high affinity for TSPO. As several steroidogenic tissues, such as the adrenal gland and testis, show high TSPO and porphyrin levels, it has been suggested a physiological role for the interaction of these two molecules. Furthermore, having a plane of symmetry, these molecules could bind dimerized form of TSPO, confirming in this way the postulated two-binding site model.[7, 15]

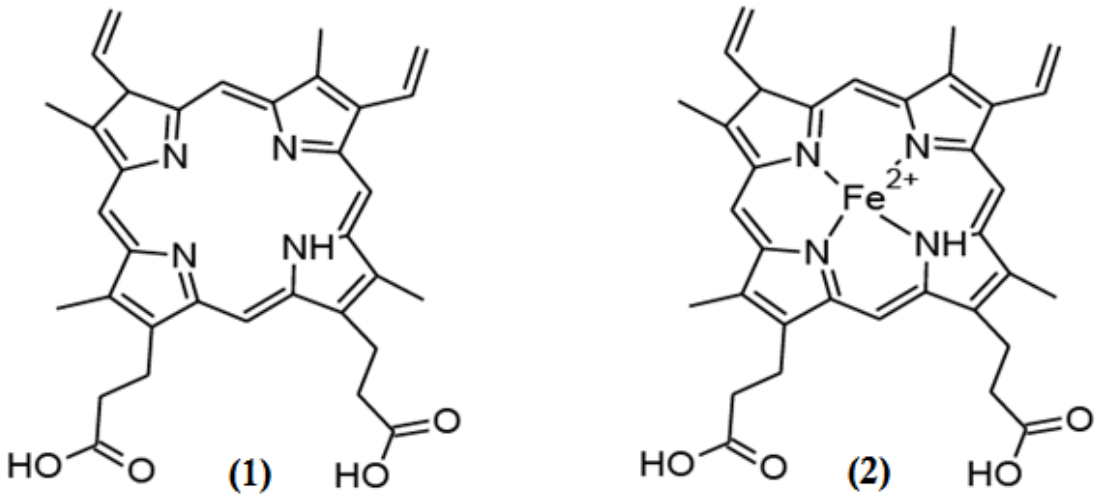

FIGURE (8): *Chemical structures of protoporphyrin IX (1) and heme (2).*

Another endogenous ligand is cholesterol, as previously reported discussing the fundamental role of TSPO in the regulation of cholesterol transport and thus in the steroidogenesis. Again it has been shown that a dimeric form of TSPO possesses an enhanced binding capacity to cholesterol. [15]

Finally, anthralin, isolated in the stomach of rat, a 16 kDa protein that has been demonstrated interact with both TSPO and dihydropyridine binding site, and phospholipase A_2 have also been proposed as endogenous ligands for TSPO. [15]

✓ *TSPO SYNTHETIC LIGANDS*

Synthetic TSPO selective ligands have been developed with the aim to deepen the knowledge of the exact pharmacological role of TSPO, to define its involvement in several patho-physiological conditions and to establish the structural requirements needed for an optimum of affinity. Initially, the most of these ligands have been designed starting from classical selective CBR ligands, such as benzodiazepines, making the necessary structural modifies in order to shift the affinity toward TSPO. Until to date, the prototypic ligands, used as reference compounds in the development of TSPO pharmacophore models and in SAR studies, are the benzodiazepine Ro 5-4864 (3) and the isoquinolinecarboxamide PK11195 (1), classified by LeFur and coworkers the first as a TSPO agonist or partial agonist and the second as an antagonist.[7]

The ligands for the TSPO not have a fixed chemical structure, but are very different among them. We can distinguish nine classes of compounds:

- In the class of ***benzodiazepines*** the selectivity toward the TSPO or CBR results very sensitive even to slight structural modifications: in fact, in the

case of Ro 5-4864 (3) the insertion of a chlorine at the para position of the pendant phenyl rings of the diazepam, equipotent at the two receptors, shifts the selectivity toward TSPO. Ro 5-4864 has been used in a number of studies aimed at characterizing TSPO, and particularly by Gavioli and colleagues to study the putative role of TSPO as a target for the treatment of psychiatric disorders.[5]

- ***Benzothiazepines***, a class of TSPO ligands featuring a 6,7 bicyclic nucleus, were initially developed by Campiani and coworkers as selective ligands for CBR and GABA receptor subtypes. Some pyrrolobenzothiazepines derivatives possess an unexpected significant inhibitory activity at L-type calcium channels, equal to or higher than those of reference calcium antagonists such as verapamil and (+)-cis-diltiazem. [5]
- On the basis of pyrrolobenzothiazepine skeleton, the ***pyrrolobenzoxazepine*** scaffold has been developed, featuring the replacement of the endocyclic sulfur (S_5) with an oxygen (O_5), that increases affinity by 2-3 fold. Some of these compounds showed an high affinity toward the TSPO (Ki values in the low nanomolar-subnanomolar range) and the capacity to stimulate steroidogenesis in mouse Y-1 adrenocortical cell line. [5]
- ***Isoquinolinecarboxamide*** PK 11195 (1) is the first non-benzothiazepine ligand binding the TSPO with nanomolar affinity and it is widely used for studies aimed to define and map the binding site. In 2008 Chelli et al.[22] showed that treatment of a human astrocytoma cell line (***ADF***) with PK 11195 actives an autophagic pathway followed by apoptosis mediated by mitochondrial potential dissipation. Moreover, has been showed that PK

11195 has a multidrug resistance modulating activity increasing the efficacy of a daunorubicin treatment on human multidrug-resistant leukemia cell line in vitro by 5-7 fold and blocking p-glycoprotein efflux, a transporter whose activity contributes to limit antitumor drug efficacy.[20]

- ***Alpidem*** (4) can be considered the progenitor of the class of imidazopyridines known to bind both TSPO and CBR with the nanomolar affinity (Ki 0.5-7 nM and 1-28 nM, respectively). [5]
- ***Phenoxyphenylacetamide*** derivatives, such as DAA1097 (9), were designed by a process of molecular simplification involving the opening of the diazepine ring of Ro 5-4864. Some compounds of this class of TSPO ligands have also showed potent anxiolytic properties in laboratory animals. [5]
- ***Pyrazolopyrimidineacetamides***, i.e. DPA714 (10), were first described by Selleri and coworkers as bioisosters of the imidazopyridines and thereby closely related to alpidem.
- ***Indoleacetamide*** derivatives, collectively named FGIN-1 (9), was developed by Kozikowski and colleagues as a new class of compounds binding with high affinity and selectivity for TSPO. [5]

  In a recent study SSR180575 (11), an indoleacetamide compound, was shown to have neuroprotective properties in different models of progressive degeneration of the PNS and CNS: precisely it promotes neuronal survival and repair following axotomy through the regulation of apoptosis of glial cells and/or the production of mediators such as neurosteroids, cytokines or other neurotrophic factors that support nerve survival.[20]

❖ ***Indol-3-ylglyoxylamides***.

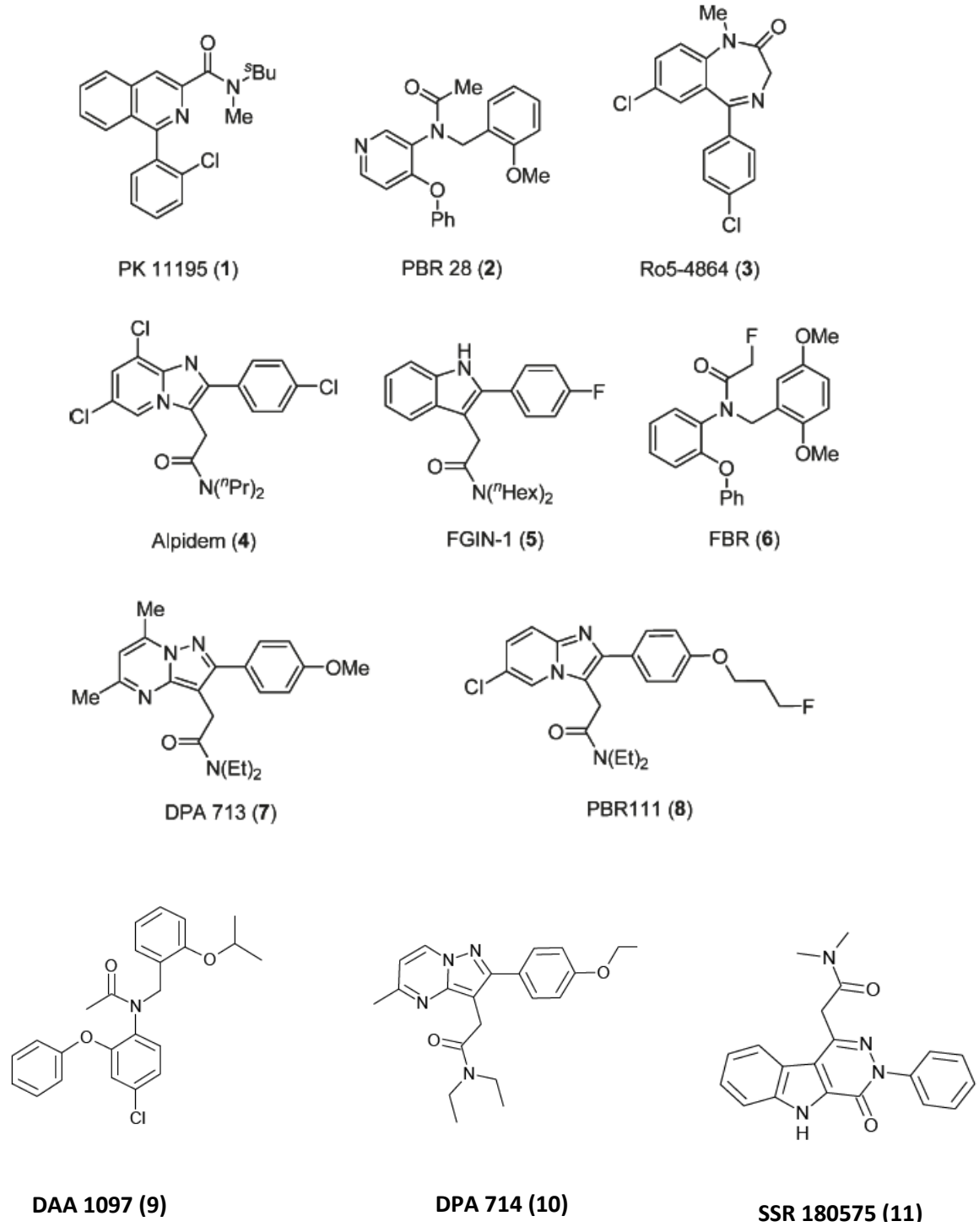

FIGURE (9): *Structures of some known TSPO ligands*

INTRODUCTION TO EXPERIMENTAL SECTION:

✓ *N,N-DIALKYL-2-PHENYLINDOL-3-YLLYOXYLAMIDES*

TSPO expression is up-regulated in several human pathologies, including gliomas and neurodegenerative disorders (Huntington's and Alzheimer's diseases) as well as in various forms of brain injury and inflammation. Under neuroinflammatory conditions, TSPO markedly increases in activated microglia.[26] Changes in TSPO level have been found in patients affected by generalized anxiety, panic, post-traumatic stress, obsessive-compulsive disorders, and separation anxiety. Consequently, TSPO has been suggested as a promising target for a number of therapeutic applications[20] and also as a diagnostic marker for related disease progression. Therefore, many groups have been searching for TSPO ligands with improved performance for quantifying TSPO expression.

Subsequently, a number of diversified structures have been developed obtaining in some cases good results in term of affinity and selectivity, and leading to drawing various TSPO pharmacophore models useful to design novel synthetic derivatives. Neverthless, the topology of the TSPO binding cleft has not yet been completely defined. In 2004 Primofiore et al.[24] prepared and tested a series of *N*,*N*-dialkyl-2-phenylindol-3-ylglyoxylamide derivatives I (***TABLE 1***) as TSPO ligands, designed as conformationally constrained analogues of the indoleacetamides of the FGIN-1 (5) series previously described by Kozikowski and coworkers. Most of these

compounds showed a high affinity for TSPO in the nanomolar / subnanomolar range and a high selectivity for TSPO over CBR. The TSPO/CBR selectivity was evaluated by binding studies using membranes from rat brain tissues and [^{3}H]flumazenil as radioligand. For some of these TSPO ligands with high affinity, the ability to stimulate pregnenolone formation from rat C6 gliomas cells was evaluated.

TABLE 1: *TSPO binding affinity of N,N-dialkylindolylglyoxylamide derivatives* **Ia-Iaah.** *[a]The concentration of tested compounds that inhibited [^{3}H-PK 11195] binding to rat kidney mitochondrial membranes (IC_{50}) by 50% was determinate with six concentrations of the displacers, each performed in triplicate. K_i values are the mean ± SEM of the three determinations. [b] the inhibition percent of [^{3}H]-flumazenil specific binding at 10μM of the compound are the mean ± SEM of five determination Ki values are the mean ± SEM of three determinations. [c] Data taken from ref. 23.*

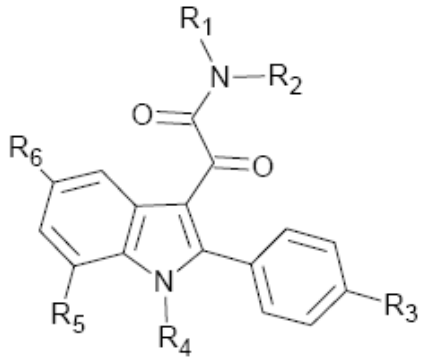

N	R_1	R_2	R_3	R_4	R_5	R_6	K_i (nM) or inhibition (%)[c]	
							TSPO [a]	CBR [b]
Ro 5-4864							23.o±3.0	
PK 11195							9.30±0.5	
Alpidem							0.5 – 7	1 -28
Ia	$(CH_2)_2CH_3$	H	H	H	H	H	815±80	3293±381
Ib	$(CH_2)_3CH_3$	H	H	H	H	H	1167±99	12%
Ic	CH_2CH_3	CH_2CH_3	H	H	H	H	43.0±4	
Id	$(CH_2)_2CH_3$	$(CH_2)_2CH_3$	H	H	H	H	12.2±1.0	16%
Ie	$(CH_2)_3CH_3$	$(CH_2)_3CH_3$	H	H	H	H	7.5±0.7	3%
If	$(CH_2)_4CH_3$	$(CH_2)_4CH_3$	H	H	H	H	16.0±2.0	3%
Ig	$(CH_2)_5CH_3$	$(CH_2)_5CH_3$	H	H	H	H	1.4±0.2	10%
Ih	$CH_2(CH_3)_2$	$CH_2(CH_3)_2$	H	H	H	H	103±9.0	
Ii	$CH(CH_3)CH_2CH_3$	$CH(CH_3)CH_2CH_3$	H	H	H	H	17.0±2.0	5%

Ij	CH_2CH_3	$CH_2C_6H_5$	H	H	H	H	11.0±1.0	
Ik	-$(CH_2)_4$-		H	H	H	H	2400±125	4%
Il	-$(CH_2)_5$-		H	H	H	H	665±30	3%
Im	-$(CH_2)_6$-		H	H	H	H	33.0±3.0	3%
In	$(CH_2)_2CH_3$	$(CH_2)_2CH_3$	F	H	H	H	4.28±0.32	4.3%
Io	$(CH_2)_3CH_3$	$(CH_2)_3CH_3$	F	H	H	H	2.40±0.81	0%
Ip	$(CH_2)_5CH_3$	$(CH_2)_5CH_3$	F	H	H	H	0.37±0.13	0%
Iq	CH_2CH_3	$CH_2C_6H_5$	F	H	H	H	1.68±0.12	10%
Ir	$(CH_2)_2CH_3$	$(CH_2)_2CH_3$	Cl	H	H	H	4.65±0.52	14%
Is	$(CH_2)_3CH_3$	$(CH_2)_3CH_3$	Cl	H	H	H	1.00±0.27	0%
It	$(CH_2)_5CH_3$	$(CH_2)_5CH_3$	Cl	H	H	H	0.55±0.19	4.2%
Iu	CH_2CH_3	$CH_2C_6H_5$	Cl	H	H	H	1.30±0.15	7.3%
Iv	$(CH_2)_2CH_3$	$(CH_2)_2CH_3$	NO_2	H	H	H	0.95±0.1	
Iw	$(CH_2)_3CH_3$	$(CH_2)_3CH_3$	NO_2	H	H	H	0.23±0.07	
Ix	$(CH_2)_5CH_3$	$(CH_2)_5CH_3$	NO_2	H	H	H	0.27±0.10	
Iy	CH_2CH_3	$CH_2C_6H_5$	NO_2	H	H	H	0.55±0.02	
Iz	$(CH_2)_2CH_3$	$(CH_2)_2CH_3$	CF_3	H	H	H	1.69±0.2	
Iaa	$(CH_2)_3CH_3$	$(CH_2)_3CH_3$	CF_3	H	H	H	1.16±0.1	
Ibb	$(CH_2)_5CH_3$	$(CH_2)_5CH_3$	CF_3	H	H	H	1.0±0.1	
Icc	CH_2CH_3	$CH_2C_6H_5$	CF_3	H	H	H	1.0±0.1	
Idd	$(CH_2)_2CH_3$	$(CH_2)_2CH_3$	CH_3	H	H	H	5.50±0.98	
Iee	$(CH_2)_3CH_3$	$(CH_2)_3CH_3$	CH_3	H	H	H	3.80±0.91	
Iff	$(CH_2)_5CH_3$	$(CH_2)_5CH_3$	CH_3	H	H	H	1.60±0.13	
Igg	CH_2CH_3	$CH_2C_6H_5$	CH_3	H	H	H	2.64±0.1	
Ihh	$(CH_2)_2CH_3$	$(CH_2)_2CH_3$	H	H	H	F	2.67±0.48	
Iii	$(CH_2)_3CH_3$	$(CH_2)_3CH_3$	H	H	H	F	4.00±0.15	
Ijj	$(CH_2)_5CH_3$	$(CH_2)_5CH_3$	H	H	H	F	0.37±0.12	
Ikk	CH_2CH_3	$CH_2C_6H_5$	H	H	H	F	1.33±0.2	
Ill	$(CH_2)_2CH_3$	$(CH_2)_2CH_3$	H	H	H	Cl	2.80±0.3	10%
Imm	$(CH_2)_3CH_3$	$(CH_2)_3CH_3$	H	H	H	Cl	4.91±0.4	13%
Inn	$(CH_2)_5CH_3$	$(CH_2)_5CH_3$	H	H	H	Cl	58.4±6	3%
Ioo	CH_2CH_3	$CH_2C_6H_5$	H	H	H	Cl	4.6±0.5	
Ipp	$(CH_2)_2CH_3$	$(CH_2)_2CH_3$	H	H	H	NO_2	20.2±2.02	0%
Iqq	$(CH_2)_3CH_3$	$(CH_2)_3CH_3$	H	H	H	NO_2	21.6±2.15	1%
Irr	$(CH_2)_5CH_3$	$(CH_2)_5CH_3$	H	H	H	NO_2	30.3±9.15	0%
Iss	CH_2CH_3	$CH_2C_6H_5$	H	H	H	NO_2	18.3±0.15	0%
Itt	$(CH_2)_2CH_3$	$(CH_2)_2CH_3$	H	H	H	OCH_3	328±45	8.6%
Iuu	$(CH_2)_3CH_3$	$(CH_2)_3CH_3$	H	H	H	OCH_3	65.2±3.4	8.8%
Ivv	$(CH_2)_5CH_3$	$(CH_2)_5CH_3$	H	H	H	OCH_3	35.5±8.7	7.3%
Iww	CH_2CH_3	$CH_2C_6H_5$	H	H	H	OCH_3	69.5±3.6	5.7%
Ixx	$(CH_2)_2CH_3$	$(CH_2)_2CH_3$	F	H	H	Cl	2.83±0.08	14%
Iyy	$(CH_2)_3CH_3$	$(CH_2)_3CH_3$	F	H	H	Cl	3.05±0.45	17%
Izz	$(CH_2)_5CH_3$	$(CH_2)_5CH_3$	F	H	H	Cl	7.75±1.55	
Iaaa	CH_2CH_3	$CH_2C_6H_5$	F	H	H	Cl	4.01±0.26	9.7%
Ibbb	$(CH_2)_2CH_3$	$(CH_2)_2CH_3$	F	H	H	F	6.73±1.39	
Iccc	$(CH_2)_3CH_3$	$(CH_2)_3CH_3$	F	H	H	F	4.36±0.05	
Iddd	$(CH_2)_5CH_3$	$(CH_2)_5CH_3$	F	H	H	F	0.95±0.1	
Ieee	CH_2CH_3	$CH_2C_6H_5$	F	H	H	F	1.67±0.37	
Ifff	$(CH_2)_2CH_3$	$(CH_2)_2CH_3$	Cl	H	H	Cl	0.62±0.06	5%
Iggg	$(CH_2)_3CH_3$	$(CH_2)_3CH_3$	Cl	H	H	Cl	1.9±0.2	0%
Ihhh	$(CH_2)_5CH_3$	$(CH_2)_5CH_3$	Cl	H	H	Cl	5.8±0.6	3%

Iiii	CH_2CH_3	$CH_2C_6H_5$	Cl	H	H	Cl	3.33±0.3	
Ijjj	$(CH_2)_2CH_3$	$(CH_2)_2CH_3$	H	H	Cl	H	14.0±1.5	0%
Ikkk	$(CH_2)_3CH_3$	$(CH_2)_3CH_3$	H	H	Cl	H	3.40±0.3	
Illl	$(CH_2)_5CH_3$	$(CH_2)_5CH_3$	H	H	Cl	H	2.4±0.3	0%
Immm	CH_2CH_3	$CH_2C_6H_5$	H	H	Cl	H	5.0±0.4	0%
Innn	$(CH_2)_2CH_3$	$(CH_2)_2CH_3$	H	H	CH_3	H	25.0±3.0	
Iooo	$(CH_2)_3CH_3$	$(CH_2)_3CH_3$	H	H	CH_3	H	6.0±0.6	
Ippp	$(CH_2)_5CH_3$	$(CH_2)_5CH_3$	H	H	CH_3	H	1.90±0.1	
Iqqq	CH_2CH_3	$CH_2C_6H_5$	H	H	CH_3	H	2.30±0.2	
Irrr	CH_3	CH_2CH_3	H	H	H	H	940±120	15%
Isss	CH_3	$(CH_2)_3CH_3$	H	H	H	H	53.3±4.0	
Ittt	CH_3	$(CH_2)_4CH_3$	H	H	H	H	12.1±1.0	
Iuuu	CH_2CH_3	$(CH_2)_3CH_3$	H	H	H	H	12.6±1.0	
Ivvv	CH_3	CH_2CH_3	Cl	H	H	Cl	9.54±1.29	15%
Iwww	CH_3	$(CH_2)_3CH_3$	Cl	H	H	Cl	0.15±0.02	
Ixxx	CH_3	$(CH_2)_4CH_3$	Cl	H	H	Cl	0.18±0.02	
Iyyy	CH_2CH_3	$(CH_2)_3CH_3$	Cl	H	H	Cl	0.36±0.04	
Izzz	CH_3	$CH_2C_6H_5$	H	H	H	H	12.0±1.0	
Iaab	CH_3	$CH_2C_6H_5$	F	H	H	H	1.8±0.1	
Iaac	CH_3	$(CH_2)_3CH_3$	Cl	H	H	H	11±1.0	
Iaad	CH_3	$(CH_2)_4CH_3$	Cl	H	H	H	3.4±0.4	
Iaae	CH_2CH_3	$(CH_2)_3CH_3$	Cl	H	H	H	3.6±0.4	
Iaaf	CH_3	$(CH_2)_3CH_3$	H	H	H	Cl	3.9±0.5	
Iaag	CH_3	$(CH_2)_4CH_3$	H	H	H	Cl	3.6±0.5	
Iaah	CH_2CH_3	$(CH_2)_3CH_3$	H	H	H	Cl	1.8±0.2	

In 2008 the same research group[16] refined the TSPO pharmacophore/topological model through the synthesis and the biological evaluation of novel indole derivatives with the general formula **I**, bearing different combinations of substituents R_1-R_6. (***TABLE 1***)

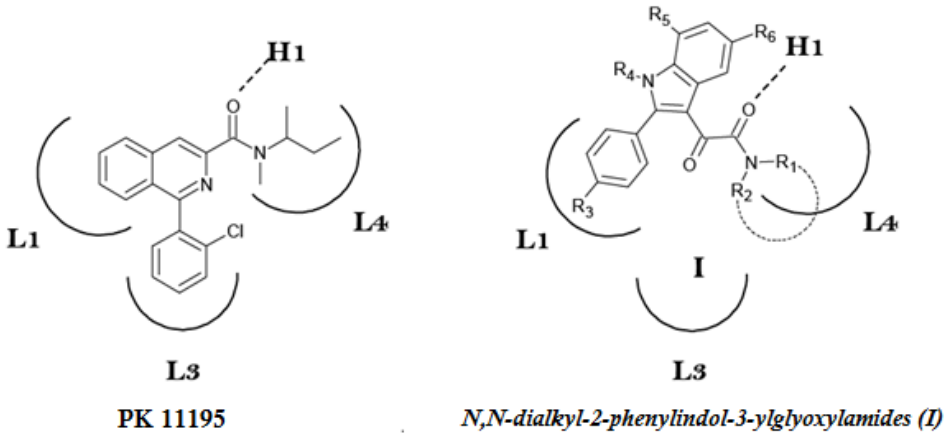

FIGURE (10): *TSPO pharmacophore/topological model.*

Within this class, SAR findings were rationalized in the light of a pharmacophore/receptor model made up of three lipophilic pockets (L1, L3, and L4) and an H-bond donor group. Specifically, the second carbonyl group of the oxalyl bridge engages an H-bond with the donor site H1; the two lipophilic substituents on the amide nitrogen, R_1, and R_2 (linear or ramified alkyl, arylalkyl groups) interact hydrophobically with the L_3 or L_4 lipophilic pockets; the 2-phenyl moiety establishes a putative π-stacking interaction within the L1 pocket. The high affinities of these 2-phenylindolglyoxylamide derivatives have recently permitted the development of new fluorescent probes useful for investigating the localization and the expression level of TSPO.[32, 26]

In ***TABLE 1*** the binding affinity of compounds **Ia**-**Iaah** [16, 24] and of the standard TSPO ligands Ro5-4864 (2), PK 11195 (5) and Alpidem (6), expressed as Ki values has been reported. It has been observed that, among the unsubstitued derivatives **Ia-Im** ($R_3 = R_4 = R_5 = R_6 = H$), N-monosubstitued compounds **Ia**-**Ib** show the lowest affinity probably because they cannot occupy both the L_3 and L_4 lipophilic pockets. The *N*,*N*-disubstitued indolylglyoxylamides instead exhibit a high affinity and in particular compound **Ig**, bearing two *n*-hexyl groups, is the most potent, with a K_i of 1,4 nM. Therefore, increasing the length of the linear *N*-alkyl groups has been observed an enhancement of affinity, due to the better filling of L_3 and L_4 lipophilic pockets.[24] Subsequently, the three derivatives **Id**, **Ie**, **Ig** and **Ij** has been selected as leads for further affinity optimization efforts. It has been observed that the insertion of an electron-donating lipophilic group, such as a methyl group (**Idd**-**Igg**), in the 4'-position (R_3) of the 2-phenyl ring does not produce any gain in affinity respect to the parent unsubstitued compound. Introducing an electron-withdrawing

substituent such as Cl, F, NO_2 and CF_3 (**In**-**Icc**), it has been instead obtained compounds with higher affinity, and among these ones, the *N*,*N*-di-*n*-hexyl derivatives **Ip** (Cl), **It** (F), **Ix** (NO2) and **Ibb** (CF_3) have been revealed the most potent, with K_i values of 0.37 nM, 0.55 nM, 0.27 nM and 1 nM, respectively. These results suggest that the R_3 substituent has to be electron-withdrawing to reinforce the putative π-stacking interaction with an electronrich aromatic ring within the L1 pocket. The data of affinity of compounds **Ihh**-**Iww** bearing a substituent in the 5-position of the indole nucleus (F, Cl, NO_2, OCH_3) suggest that R_6 has to be electron-withdrawing and also very small for optimal binding, and only **Ijj** with a fluorine at the 5-position features these properties (K_i = 0.37 nM). The introduction of two halogens in both 4'- and 5-positions (**Ixx**-**Iiii; Ivvv**-**Iyyy**) does not increase affinity in additive manner, but it has supposed a correlation with the nature of the *N*,*N*-dialkyl chain. Substitutions at the 7-position of the indole nucleus (R_5) with an electron-withdrawing (Cl, **Ijjj**-**Immm**) or an electron-donating (CH_3, **Innn**-**Iqqq**) lipophilic group do not produce any gain in affinity.

The binding data of asymmetrical *N*,*N*-dialkyl derivatives (**Irrr**-**Iaah**), designed to probe the L_3 and L_4 lipophilic pockets at the TSPO binding site, indicate that the L_3 and L_4 pockets are probably different in their dimensions, and that R_1 and R_2 have to be of different size to obtain the best-performing substitution on the amide nitrogen. Therefore, an aromatic moiety on R_1/R_2 substituents is equivalent to an aliphatic moiety of similar size in interacting with the two lipophilic pockets.

In the light of all these findings, research is currently focused towards the synthesis and biological evaluation of a series of *N,N-dialkyl-2-phenylindol-3-ylglyoxylamides* (**II**) bearing a polar group at the 4'-position of the 2-phenyl ring (R_3 = NH_2, OH,

COOH), and of a series of *N*,*N*-dialkyl-2-(3-thienyl)indol-3-ylglyoxylamides (**III**). These compounds have been synthesized as symmetrical amides featuring linear alkyl chains of different length on the amide nitrogen (*n*-propyl, *n*-butyl, *n*-hexyl) to evaluate any changes in the interaction with the lipophilic pockets L3, L4 of the pharmacophore. The TSPO affinity of intermediary compounds featuring a OCH_3 and a $COOCH_3$ substituent in 4'-position has also been estimated.

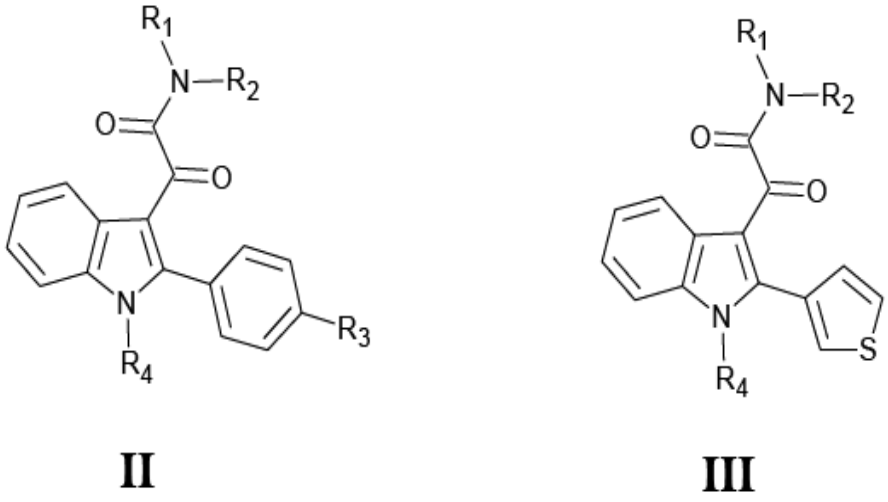

FIGURE(11): *Chemical structures of N,N-dialkyl-2-phenylindol-3-ylglyoxylamides (II) and N,N-dialkyl-2-(3-thienyl)indol-3-ylglyoxylamides (III).*

To make these molecules are used as potential drugs or radiopharmaceuticals (as biomarkers of neuroinflammation), they must have a good pharmacokinetic profile. Therefore, the choice to insert a polar group in the scaffold of *indolylglyoxylamide* derivatives has the purpose to improve the lipophilic/hydrophilic balance, thus avoiding a high level of non-specific binding, a poor signal-to-noise ratios, a high plasma protein binding and thus a relatively poor penetration of the blood-brain barrier, resulting in accumulation of tracer in the brain.

EXPERIMENTAL SECTION:

In this thesis work compounds **29**, **30**, **31** (2-(3-thienyl)), **31**, **32** (R_3 = NH_2), **35**, **36** (R_3 = OH), **37**, **38**, **39** (R_3 = COOH). It has also been estimated the K_i value of **20**, **21, 22** (R_3 = OMe), **23**, **24** , **25**, (R_3 = COOMe) were prepared and biologically evaluted.

The general synthetic procedures employed to prepare these compounds are shown in **Scheme 1** and **2**. They involve, as first step, the synthesis of the 2-phenylindoles **16a-c** and 2-(3-thienyl) indole **27** through a one-step Fischer indole synthesis[16] consisting in warming phenylhydrazine hydrochloride and the appropriate ketone acetophenone, methyl 4-acetylbenzoate, acetylthiophene directly with an excess of acid catalyst PPA (polyphosphoric acid). The reaction mixture was then poured into ice and the solid precipitated was collected by filtration and purified by recrystallization from toluene.

Scheme 1:

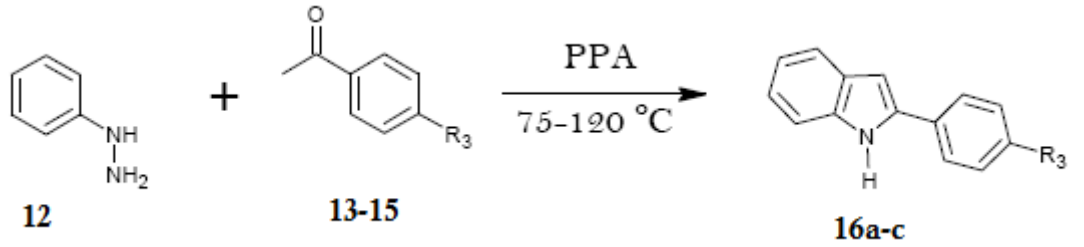

12 13-15 16a-c

n	R_3
16a; 17a	NO_2
16b; 17b	OCH_3
16c; 17c	COOMe

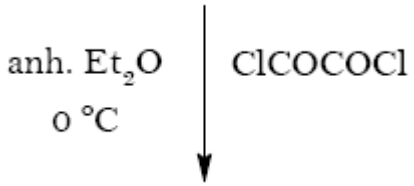

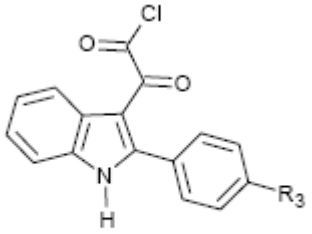

17a-c

n	$R_1 = R_2$	R_3
1v	$(CH_2)_2CH_3$	NO_2
18	$(CH_2)_3CH_3$	NO_2
19	$(CH_2)_5CH_3$	NO_2
20	$(CH_2)_2CH_3$	OMe
21	$(CH_2)_3CH_3$	OMe
22	$(CH_2)_5CH_3$	OMe
23	$(CH_2)_2CH_3$	COOMe
24	$(CH_2)_3CH_3$	COOMe
25	$(CH_2)_5CH_3$	COOMe

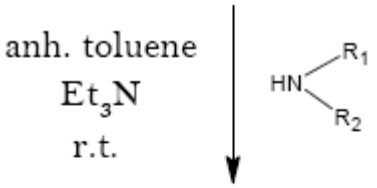

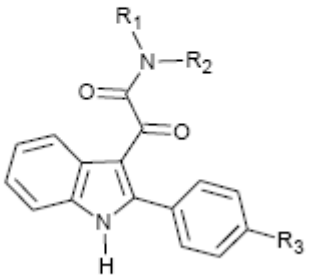

1v, 18-25

The indoles **16a-c** and **27** were then acylated with oxalyl chloride in anhydrous ethyl ether at 0°C to give the corresponding indolylglyoxylyl chlorides **17a-c** and **28**, which were allowed to react in dry toluene solution and nitrogen atmosphere with the appropriate amine, in presence of triethylamine in equimolar quantity to neutralize the hydrochloridric acid formed during the reaction of condensation.[24] The crude compounds, after washing with a solution of 5% $NaHCO_3$ dil. and then with H_2O to eliminate the amine not reacted, with HCl dil. 10% and again H2O to remove the excess of Et_3N, were tritured at 0°C with ethylether to yield the indolylglyoxylamides **1v**, **18-24**, and **29**, **30**. Their chemical-physical properties were determined, and their structures were confirmed by ^{1}H-NMR. (***TABLE 2)***

Scheme 2:

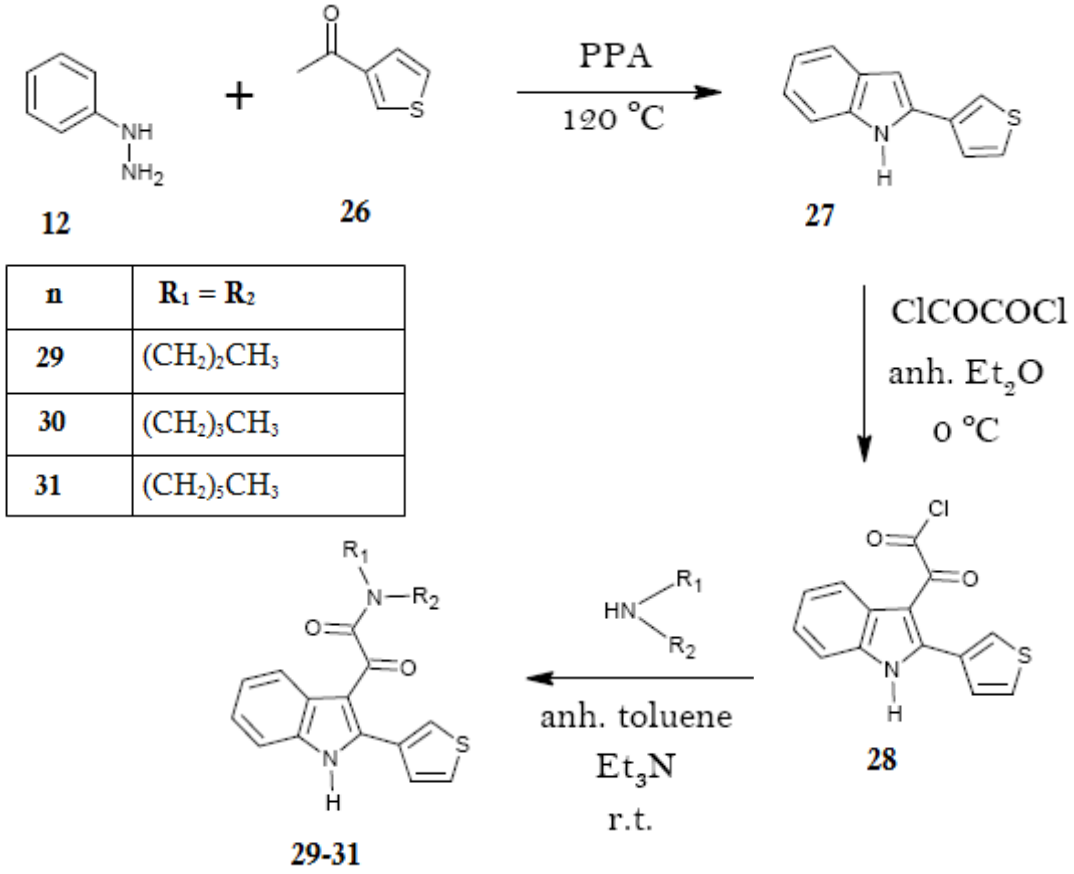

12 + 26 → 27 → 28 → 29-31

n	$R_1 = R_2$
29	$(CH_2)_2CH_3$
30	$(CH_2)_3CH_3$
31	$(CH_2)_5CH_3$

The synthesis of the target compounds **32** and **33** ($R_3 = NH_2$), **35** and **36** ($R_3 = OH$), and **38**-**40** ($R_3 = COOH$) was achieved by the procedures outlined in **Schemes 3**, **4** and **5**. Briefly starting by indoles, previously prepared **1v**, **18**-**25**, we obtain, through appropriate reactions, the corresponding compounds featuring a polar group at the 4'-position of the 2-phenyl ring.

Scheme 3:

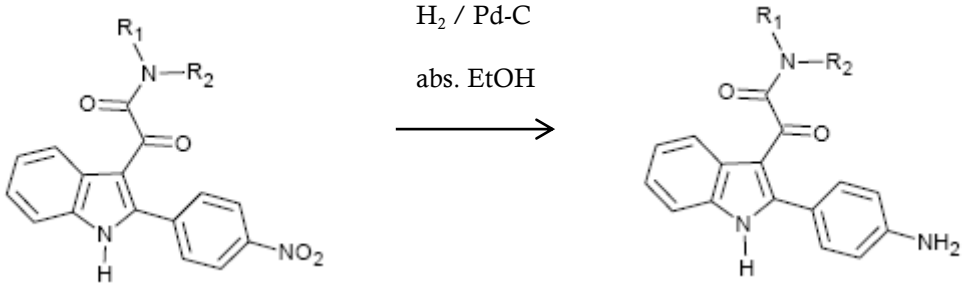

1v, **18, 19** **32, 33, 34**

The **Scheme 3** describes the general procedure for the synthesis of the 2-phenylindolylglyolamide derivatives bearing a NH_2 at para position at the 2-phenyl ring:[26] *N*,*N*-dialkyl-[2-(4-nitrophenyl)indol-3-yl]glyoxylamide derivatives **1v, 18** and **19** were catalytically hydrogenated over palladium to yield the relative amines **32, 33** and **34**. Their chemical-physical properties and ^{1}H-NMR data are reported in ***TABLE 2***.

Scheme 4:

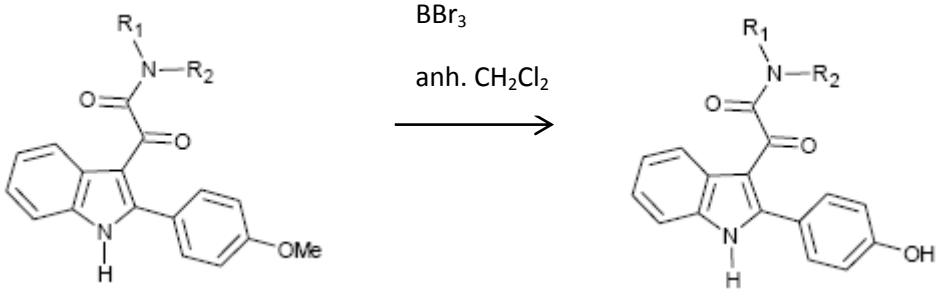

20-22 **35, 36**

The indolylglyoxylamide derivatives featuring a OH group at R_3 (**35, 36**) were obtained through a demethylation of the corresponding methoxy compounds **20** - **22**[34] (**Scheme 4**) by treatment with BBr_3, in anhydrous dichloromethane, in a nitrogen atmosphere. At the end of the reaction (TLC analysis), methanol was added to the mixture to hydrolyze the excess of BBr_3, and crude compounds **35**, **36** were recovered as a solid precipitated after evaporation of the solvent under reduced pressure. Their chemical-physical properties and ^{1}H-NMR data are reported in ***TABLE 2***.

Scheme 5 report the synthetic procedure to obtain compounds **37** - **39** by hydrolysis of the methyl ester[35] of methyl 4-(3-dialkyl-aminoglyoxylylindol-2-yl)benzoate derivatives **23**–**25** by treatment with lithium hydroxide monohydrate to a MeOH/H_2O (3:1) solution. The chemical-physical properties and ^{1}H-NMR data of derivatives **23**–**25** are reported in ***TABLE 2***.

Scheme 5:

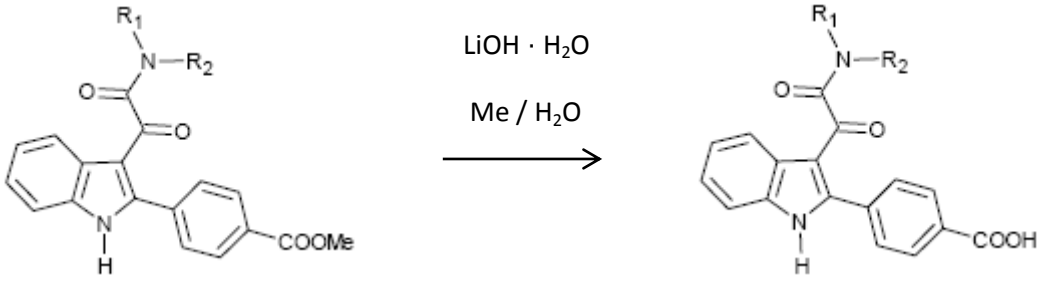

23 –25 **37 – 39**

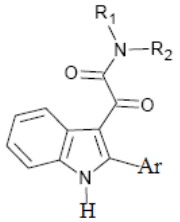

TABLE 2 Yields, melting points, and spectral data of compounds **20–25** *and* **29-39:**

n	$R_1 = R_2$	Ar	Yeld (%)	mp (C°) (cristallization solvent)	1H-NMR (DMSO – *d6*, ppm)	Formula
20	$(CH_2)_2CH_3$	*p*-OCH_3-C_6H_4	52	121-126 (toluene)	0.64-0.79 (m, 6H, $CH_2CH_2CH_3$); 1.21-1.26 (m, 2H,$CH_2CH_2CH_3$); 1.39-1.47 (m, 2H,$CH_2CH_2CH_3$);2.93-3.06 (2t, 4H, J=7 Hz, $CH_2CH_2CH_3$);3.83 (s, 3H, OCH_3); 7.06 (d, 2H, J=8 Hz, ArH);7.08-7.29(m, 2H, ArH); 7.42 (d, 1H, J=8 Hz, ArH);7.50(d, 2H, J=8 Hz, ArH);8.01(d, 1H, J=8 Hz, ArH);12.34(S, 1H, NH exch. with D_2O).	$C_{23}H_{26}N_2O_3$
21	$(CH_2)_3CH_3$	*p*-OCH_3-C_6H_4	55	117-121 (toluene)	0.68-0.85 (m, 6H, $CH_2CH_2CH_2CH_3$); 1.02-1.10 (m, 4H, $CH_2CH_2CH_2CH_3$); 1.13-1.41 (m, 4H, $CH_2CH_2CH_2CH_3$); 2.99-3.03 (2t, 4H, J=7 Hz, $CH_2CH_2CH_2CH_3$); 3.83 (1s, 3H, OCH_3); 7.06 (d, 2H, J=8 Hz, ArH); 7.20-7.28 (m, 2H, ArH); 7.46 (d, 1H, J=8 Hz, ArH); 7.53 (d, 2H, J=8 Hz, ArH); 8.05 (d, 1H, J=8 Hz, ArH); 12.53 (S, 1H, NH	$C_{25}H_{30}N_2O_3$
22	$(CH_2)_5CH_3$	*p*-OCH_3-C_6H_4	45	oil	0.73-0.86 (2t, 6H, J=7 Hz, $CH_2CH_2CH_2CH_2CH_2CH_3$); 1.04-1.21 (m, 12H, $CH_2CH_2CH_2CH_2CH_2CH_3$); 2.98-3.05 (m, 4H, $CH_2CH_2CH_2CH_2CH_2CH_3$); 3.68-3.71 (m, 4H, $CH_2CH_2CH_2CH_2CH_2CH_3$); 3.83 (1s, 3H, OCH_3); 7.05 (d, 2H, J=7 Hz, ArH); 7.20-7.25 (m, 2H, ArH); 7.45 (d, 1H, J=6 Hz, ArH); 7.53 (d, 2H, J=7 Hz, ArH); 8.02 (d, 1H, J=6 Hz, ArH); 12.33 (S, 1H, NH exch. with D_2O).	$C_{29}H_{38}N_2O_3$

n	$R_1 = R_2$	Ar	Yeld (%)	mp (C°) (cristallization solvent)	1H-NMR (DMSO – *d6*, ppm)	Formula
23	$(CH_2)_2CH_3$	*p*-$COOCH_3$-C_6H_4	65	139-141 (toluene)	0.66-0.77 (m, 6H, $CH_2CH_2CH_3$); 1.20-1.27 (m, 2H, $CH_2CH_2CH_3$); 1.45-1.49 (m, 2H, $CH_2CH_2CH_3$); 2.93-3.10 (2t, 4H, J=8 Hz, $CH_2CH_2CH_3$); 3.92 (1s, 3H, $COOCH_3$); 7.27-7.31 (m, 2H, ArH); 7.52 (d, 1H, J=8 Hz, ArH); 7.74 (d, 2H, J=8 Hz, ArH); 8.02-8.09 (m, 3H, ArH); 12.64 (S, 1H, NH exch. with D_2O).	$C_{24}H_{26}N_2O_4$
24	$(CH_2)_3CH_3$	*p*-$COOCH_3$-C_6H_4	61	119-121 (toluene)	0.69-0.80 (m, 6H, $CH_2CH_2CH_2CH_3$); 1.00-1.15 (m, 4H, $CH_2CH_2CH_2CH_3$); 1.25-1.41 (m, 4H, $CH_2CH_2CH_2CH_3$); 2.95-3.09 (2t, 4H, J=7 Hz, $CH_2CH_2CH_2CH_3$); 3.89 (1s, 3H, $COOCH_3$); 7.25-7.30 (m, 2H, ArH); 7.49 (d, 1H, J=8 Hz, ArH); 7.72 (d, 2H, J=8 Hz, ArH); 8.04-8.09 (m, 3H, ArH); 12.59 (S, 1H, NH exch. with D_2O).	$C_{26}H_{30}N_2O_4$
25	$(CH_2)_5CH_3$	*p*-$COOCH_3$-C_6H_4	55	oil	0.66-0.77 (2t, 6H, J=7 Hz, $CH_2CH_2CH_2CH_2CH_2CH_3$); 0.98-1.17 (m, 12H, $CH_2CH_2CH_2CH_2CH_2CH_3$); 1.32-1.46 (m, 4H, $CH_2CH_2CH_2CH_2CH_2CH_3$); 2.85-2.97 (m, 4H, $CH_2CH_2CH_2CH_2CH_2CH_3$); 3.81 (1s, 3H, $COOCH_3$); 7.18-7.21 (m, 2H, ArH); 7.40 (d, 1H, J=7 Hz, ArH); 7.64 (d, 2H, J=8 Hz, ArH); 7.96-8.00 (m, 3H, ArH); 12.53 (S, 1H, NH exch. with D_2O).	$C_{30}H_{38}N_2O_4$
29	$(CH_2)_2CH_3$	thiophene	78	68 -71 (toluene)	0.65 (t, 3H, J=8 Hz, $CH_2CH_2CH_3$); 0.81 (t, 3H, J=8 Hz, $CH_2CH_2CH_3$); 1.30-1.50 (m, 4H, $CH_2CH_2CH_3$); 3.00-3.14 (m, 4H, $CH_2CH_2CH_3$); 7.21-7.27 (m, 2H, ArH); 7.46-7.50 (m, 2H, ArH); 7.69-7.73 (m, 1H, ArH); 7.91 (d, 1H, J=7 Hz, ArH); 8.13 (d, 1H, J=2 Hz, ArH); 12.45 (S, 1H, NH exch. with D_2O).	$C_{20}H_{22}N_2O_2S$

n	$R_1 = R_2$	Ar	Yeld (%)	mp (C°) (cristallization solvent)	1H-NMR (DMSO – *d6*, ppm)	Formula
30	$(CH_2)_3CH_3$	thiophene	79	118-121 (toluene)	0.66 (t, 3H, J=7 Hz, $CH_2CH_2CH_2CH_3$); 0.89 (t, 3H, J=7 Hz, $CH_2CH_2CH_2CH_3$); 0.98.-1.09 (m, 4H, $CH_2CH_2CH_2CH_3$); 1.21-1.36 (m, 4H, $CH_2CH_2CH_2CH_3$); 3.00-3.19 (2t, 4H, J=8 Hz, $CH_2CH_2CH_2CH_3$); 7.16-7.30 (m, 2H, ArH); 7.45-7.49 (m, 2H, ArH); 7.68-7.72 (m, 1H, ArH); 7.90 (d, 1H, J=8 Hz, ArH); 8.11 (S, 1H, ArH); 12.43 (S, 1H, NH exch. with D_2O).	$C_{22}H_{26}N_2O_2S$
31	$(CH_2)_5CH_3$	thiophene	82	oil	0,66-0.72 (m, 3H, CH3); 0.87-1.12 (m, 11H, 5CH2CH3); 1,26-1.39 (m, 8H, 4CH2); 3.00-3.20 (m, 4H, 2CH2); 7.18-7.29 (m, 2H, ArH); 7.45-7.51 (m, 2H, ArH); 7.68-7.72 (m, 1H, ArH); 7.87-7.93 (m, 1H, ArH); 8.14 (S, 1H, ArH); 12.44 (bs, exch. with D2O, 1H, NH);	$C_{26}H_{33}N_2O_2S$
32	$(CH_2)_2CH_3$	*p*-NH_2- C_6H_4	52	197-198 (toluene)	0.63-0.84 (m, 6H, $CH_2CH_2CH_3$); 1.29-1.37 (m, 2H, $CH_2CH_2CH_3$); 1.41-1.49 (m, 2H, $CH_2CH_2CH_3$); 2.97-3.08 (2t, 4H, J=7 Hz, $CH_2CH_2CH_3$); 5.57 (s, 2H, NH_2 exch. with D_2O); 6.62 (d, 2H, J=8 Hz, ArH); 7.17-7.43 (m, 5H, ArH); 7.92-7.97 (m, 1H, ArH); 12.09 (S, 1H, NH exch. with D_2O).	$C_{22}H_{25}N_3O_2$
33	$(CH_2)_3CH_3$	*p*-NH_2- C_6H_4	61	224-227 (toluene)	0.64-0.89 (m, 6H, $CH_2CH_2CH_2CH_3$); 0.98-1.00 (m, 4H, $CH_2CH_2CH_2CH_3$); 1.20-1.36 (m, 4H, $CH_2CH_2CH_2CH_3$); 3.00-3.06 (2t, 4H, J=7 Hz, $CH_2CH_2CH_2CH_3$); 5.52 (s, 2H, NH_2 exch. with D_2O); 6.61 (d, 2H, J=8 Hz, ArH); 7.15-7.21 (m, 2H, ArH); 7.28 (d, 2H, J=8 Hz, ArH); 7.39 (d, 1H, J=7 Hz, ArH); 7.94 (d, 1H, J=7 Hz, ArH); 12.08 (S, 1H, NH exch. with D_2O).	$C_{24}H_{29}N_3O_2$

n	$R_1 = R_2$	Ar	Yeld (%)	mp (C°) (cristallization solvent)	1H-NMR (DMSO – *d6*, ppm)	Formula
34	$(CH_2)_5CH_3$	*p*-NH_2- C_6H_4	58	147-149 (toluene	0.60-0.66 (m, 3H, CH_3); 0.82-0.93 (m, 11H, 5CH2CH3); 1.20-1.24 (m, 8H, 4CH2); 2.97-3.12 (m, 4H, 2CH2); 5.58 (bs, exch. with D_2O, 2H, NH2); 6.60 (d, 1H, ArH, J=8.6 Hz); 7.16-7.41 (m, 6H, ArH); 7.91 (d, 1H, ArH, J=7Hz); 12.08 (bs, exch. with D_2O, 1H, NH);	$C_{30}H_{37}N_3O_2$
35	$(CH_2)_2CH_3$	*p*-OH- C_6H_4	59	210-212 (toluene)	0.64-0.82 (m, 6H, $CH_2CH_2CH_3$); 1.27-1.46 (m, 4H, $CH_2CH_2CH_3$); 2.95-3.02 (2t, 4H, J=8 Hz, $CH_2CH_2CH_3$); 6.86 (d, 2H, J=8 Hz, ArH); 7.17-7.25 (m, 2H, ArH); 7.40 (d, 3H, J=8 Hz, ArH); 8.01 (d, 1H, J=7 Hz, ArH); 9.89 (s, 1H, OH exch. with D_2O); 12.27 (s, 1H, NH exch. with D_2O).	$C_{22}H_{24}N_2O_3$
36	$(CH_2)_3CH_3$	*p*-OH- C_6H_4	68	249-252	0.68-0.84 (m, 6H, $CH_2CH_2CH_2CH_3$); 1.02-1.14 (m, 4H, $CH_2CH_2CH_2CH_3$); 1.21-1.36 (m, 4H, $CH_2CH_2CH_2CH_3$); 2.94-2.98 (2t, 4H, J=7 Hz, $CH_2CH_2CH_2CH_3$); 6.83 (d, 2H, J=7 Hz, ArH); 7.19-7.21(m, 2H, ArH); 7.37-7.40 (m, 3H, ArH); 7.98 (d, 1H, J=7 Hz, ArH); 9.84 (s, 1H, OH exch. with D_2O); 12.22 (s, 1H, NH exch. with D_2O).	$C_{24}H_{28}N_2O_3$
37	$(CH_2)_2CH_3$	*p*-COOH-C_6H_4	85	292-294	0.64-0.75 (m, 6H, $CH_2CH_2CH_3$); 1.15-1.26 (m, 2H, $CH_2CH_2CH_3$); 1.43-1.47 (m, 2H, $CH_2CH_2CH_3$); 2.88-3.15 (2t, 4H, J=8 Hz, $CH_2CH_2CH_3$); 7.27-7.31 (m, 2H, ArH); 7.51 (d, 1H, J=8 Hz, ArH); 7.71 (d, 2H, J=8 Hz, ArH); 8.04 (d, 3H, J=8 Hz, ArH); 12.63 (s, 1H, NH exch. with D_2O).	$C_{23}H_{24}N_2O_4$

n	$R_1 = R_2$	Ar	Yeld (%)	mp (C°) (cristallization solvent)	1H-NMR (DMSO – *d6*, ppm)	Formula
38	$(CH_2)_3CH_3$	*p*-COOH-C_6H_4	87	147-150	0.68-0.80 (m, 6H, $CH_2CH_2CH_2CH_3$); 1.03-1.08 (m, 4H, $CH_2CH_2CH_2CH_3$); 1.10-1.40 (m, 4H, $CH_2CH_2CH_2CH_3$); 2.93-3.04 (2t, 4H, J=7 Hz, $CH_2CH_2CH_2CH_3$); 7.25-7.28 (m, 2H, ArH); 7.48 (d, 1H, J=7 Hz, ArH); 7.68 (d, 2H, J=7 Hz, ArH); 8.00-8.07 (m, 3H, ArH); 12.56 (s, 1H, NH exch. with D_2O).	$C_{25}H_{28}N_2O_4$
39	$(CH_2)_5CH_3$	*p*-COOH-C_6H_4	79	241-244	0.73-0.84 (2t, 6H, J=7 Hz, $CH_2CH_2CH_2CH_2CH_2CH_3$); 1.00-1.12 (m, 12H, $CH_2CH_2CH_2CH_2CH_2CH_3$); 1.27-1.39 (m, 4H, $CH_2CH_2CH_2CH_2CH_2CH_3$); 2.93-3.03 (m, 4H, $CH_2CH_2CH_2CH_2CH_2CH_3$); 7.24-7.27 (m, 2H, ArH); 7.48 (d, 1H, J=7 Hz, ArH); 7.68 (d, 2H, J=8 Hz, ArH); 8.00-8.05 (m, 3H, ArH); 12.56 (s, 1H, NH exch. with D_2O).	$C_{29}H_{36}N_2O_4$

✓ *MATERIALS AND METHODS:*

Melting points were determined using a Reichert Köfler hot-stage apparatus and are uncorrected. Routine nuclear magnetic resonance spectra were recorded in DMSO-d_6 solution on a Varian Gemini 200 spectrometer operating at 200 MHz. Evaporation was performed in vacuo (rotary evaporator). Analytical TLC was carried out on Merck 0.2 mm precoated silica gel aluminum sheets (60 F-254). Silica gel 60 Merck (230-400 mesh ASTM) was used for column chroma-tography. Anhydrous reactions were performed in flame-dried glassware under N2. All compounds showed ≥ 95% purity. All reagents used were obtained from commercial sources. All solvents were of an analytical grade.

✓ *CHEMISTRY:*

General procedure for the synthesis of:

2-phenyl-1H-indole derivatives (**16a**, **16b**), methyl 4-(1H-indol-2-yl)benzoate derivative (**16c**), 2-(3-thienyl)-1H-indole derivative (**27**):

1 g of polyphosphoric acid (PPA) was added to a mixture of phenylhydrazine chlorhydrate (5.0 mmol) and methyl 4-acetylbenzoate (5.0 mmol), or the appropriate acetophenone (5.0 mmol), or acetylthiophene (5.0 mmol). The reaction was maintained at 75°C for 30 min for **16a** (TLC analysis: petroleum ether/ethyl acetate, 7:3), at 120°C for 4 h for **16b** (TLC analysis: toluene/acetonitrile, 9:1) and **27** (TLC analysis: chloroform), and at 60°C for 4 h for compound **16c** (TLC analysis: chloroform). When the starting material was disappeared, the reaction

mixture was poured into ice and the precipitated solid was collected by filtration. All products were purified by recrystallization from toluene.

Yield, melting point, and spectral data of compound **16a** were reported in literature.[16]

2-(4-methoxyphenyl)-1H-indole (**16b**). Yield: 84%; m. p.: 231-234 °C; ^{1}H-NMR (DMSO-d_6, ppm): 3.80 (s, 3H, OCH_3); 6.76 (d, 1H, J = 1.8 Hz, ArH); 6.96-7.09 (m, 4H, ArH); 7.36 (d, 1H, J = 8 Hz, ArH); 7.49 (d, 1H, J = 7.2 Hz, ArH); 7.77-7.81 (m, 2H, ArH); 11.40 (s, 1H, NH exch. with D_2O).

Methyl 4-(1H-indol-2-yl)benzoate (**16c**). Yield: 78%; m. p.: 204-207 °C; 1H-NMR (DMSO-d_6, ppm): 3.87 (s, 3H, $COOCH_3$); 7.02-7.15 (m, 3H, ArH); 7.43 (d, 1H, J=8 Hz, ArH); 7.57 (d, 1H, J=8 Hz, ArH); 8.02 (s, 4H, ArH); 11.73 (s, 1H, NH exch. with D_2O).

2-(3-thienyl)-1H-indole (**27**). Yield: 89%; m. p.: 243-245 °C; 1H-NMR (DMSO-d_6, ppm): 6.76 (d, 1H, J = 0.8 Hz, ArH); 6.94-7.12 (m, 2H, ArH); 7.37 (d, 1H, J = 8 Hz, ArH); 7.51 (d, 1H, J = 8 Hz, ArH); 7.59-7.67 (m, 2H, ArH); 7.87 (t, 1H, J = 1.5 Hz, ArH).

General procedure for the synthesis of:

(2-phenylindol-3-yl)glyoxylyl chloride derivatives (**17a, 17b**), methyl 4-(3-chloroglyoxylylindol-2-yl)benzoate derivative (**17c**), [2-(3-thienyl)indol-3-yl]glyoxylyl chloride derivative (**28**):

Oxalyl chloride (8.0 mmol) was added dropwise at 0°C to a well-stirred mixture of the appropriate indole **16a-c** or **27** (4.0 mmol) in freshly distilled diethyl ether (10 mL). The mixture was maintained at room temperature for 2-24 h (TLC analysis: chloroform). A solid precipitate was obtained in the case of compounds **17b** and

17c, which was collected by vacuum filtration, and immediately used in the subsequent reaction. Instead, starting by compounds **16a** and **27**, it was not observed any formation of precipitate: thus, the solvent of reaction was evaporated under reduced pressure, and the generated solid was washed with portions of anhydrous diethyl ether to give the correspondent acyl chlorides **17a** and **28**.

[2-(4-nitrophenyl)indol-3-yl]glyoxylyl chloride (**17a**). Yield: 60%

[2-(4-methoxyphenyl)indol-3-yl]glyoxylyl chloride (**17b**). Yield: 72%

Methyl 4-(3-chloroglyoxylylindol-2-yl)benzoate (**17c**). Yield: 80%

[2-(3-thienyl)indol-3-yl]glyoxylyl chloride (**28**). Yield: 65%

General procedure for the synthesis of:

N,*N*-dialkyl-(2-phenylindol-3-yl)glyoxylamide derivatives (**1v**, **18**-**22**), methyl 4-(3-dialkylaminoglyoxylylindole-2-yl)benzoate derivatives (**23**-**25**), *N*,*N*-dialkyl-[2-(3-thienyl)indol-3-yl]glyoxylamide derivatives (**29**, **30**, **31**):

A solution of an appropriate ammine (2.0 mmol) in 5 mL of dry toluene was added dropwise to a stirred suspension, cooled at 0°C, of the (2-phenylindol-3-yl)glyoxylyl chloride derivatives **17a, 17b** (2.0 mmol), or methyl 4-(3-chloroglyoxylylindol-2-yl)benzoate derivative **17c** (2.0 mmol), or [2-(3-thienyl)indol-3-yl]glyoxylyl chloride derivative **28** (2.0 mmol) in 50 mL of the same solvent, followed by the addition of a solution of triethylamine (2.0 mmol). The reaction mixture was left under stirring for 2-24 h at room temperature (TLC analysis with appropriate eluent), and then filtered. The collected precipitate was triturated with a $NaHCO_3$ 5% aqueous solution, washed with water, and collected again to give a first portion of crude product. The toluene solution was instead removed under reduced pressure, and the oily residue obtained was extracted with $CHCl_3$ and purified by washing with 1) a

solution of $NaHCO_3$ dil. 5%; 2) H_2O; 3) HCl dil. 10%; and finally 4) H_2O. After drying with $MgSO_4$, the chloroform solution was evaporated to dryness, and the residue was tritured at 0 °C with ethylic ether to yield the crude product, that was collected by filtration. In the case of less soluble products, the crude compound precipitates together with the triethylamine hydrochloride and was collected, after washing with a solution of $NaHCO_3$ dil. 5%, and dried over P_2O_5 in vacuo.

All products generally did not require additional purification steps, but in the case of dirty compounds they were purified by recrystallization from toluene; only the compound **1v**, *N*,*N*-di-n-propyl-[2-(4-nitrophenyl)indol-3-yl]glyoxylamide, was purified by flash chromatography ($CHCl_3$ as eluent), as reported in literature.[16] Yields, melting points, and spectral data are listed in ***TABLE 2***.

Yield, melting point, and spectral data of compound *N*,*N*-di-n-propyl-[2-(4-nitrophenyl)indol-3-yl]glyoxylamide were reported in literature.[16, 24]

N,*N*-di-n-butyl-[2-(4-nitrophenyl)indol-3-yl]glyoxylamide (**18**).

Yield: 57%; m. p.: 201-203 °C; 1H-NMR (DMSO-d_6, ppm): 0.70-0.78 (m, 6H, $CH_2CH_2CH_2CH_3$); 0.97-1.20 (m, 4H, $CH_2CH_2CH_2CH_3$); 1.32-1.53 (m, 4H, $CH_2CH_2CH_2CH_3$); 3.07 (2t, 4H, J=8 Hz, $CH_2CH_2CH_2CH_3$); 7.22-7.37 (m, 2H, ArH); 7.54 (d, 1H, J=7 Hz, ArH); 7.89 (d, 2H, J=8 Hz, ArH); 8.05 (d, 1H, J=7 Hz, ArH); 8.38 (d, 2H, J=8 Hz, ArH); 12.74 (s, 1H, NH exch. with D_2O).

N,*N*-di-n-hexyl-[2-(4-nitrophenyl)indol-3-yl]glyoxylamide (**19**).

Yield: 60%; m. p.: 219-221 °C; 1H-NMR (DMSO-d_6, ppm): 0.70-0.82 (m, 3H, $2CH_3$); 1.06-1.40 (m, 16H, $8CH_2$); 2.99-3.07 (m, 4H, $2CH_2$); 7.28-7.31 (m, 2H, ArH); 7.50-7.53 (m, 1H, ArH); 7.84-7.89 (m, 2H, ArH); 8.01-8.03 (m, 1H, ArH); 8.31-8.37 (m, 2H, ArH); 12.72 (bs, exch with D_2O, 1H, NH).

General procedure for the synthesis of:

N,*N*-dialkyl-[2-(4'-aminophenyl)indol-3-yl]glyoxylamide derivatives (**32-34**):

Pd/C 10% (0.05 g) was added to a suspension of the appropriate *N*,*N*-dialkyl-[2-(4'-aminophenyl)indol-3-yl]glyoxylamide derivatives **1v** or **18** (0.65 mmol) in 150 mL of absolute ethanol. The mixture was hydrogenated under stirring for 5 h at room temperature and reduced pressure (TLC analysis with appropriate eluent). Once hydrogen absorption ceased, the catalyst was filtered off and the ethanolic solution was evaporated to dryness at reduced pressure. All products were purified by recrystallization from toluene. Yields, melting points, and spectral data of compounds **32-34** are listed in ***TABLE 2***.

General procedure for the synthesis of:

N,*N*-dialkyl-[2-(4'-hydroxyphenyl)indol-3-yl]glyoxylamide derivatives (**35-36**)

To a stirred suspension of *N*,*N*-dialkyl-[2-(4-methoxyphenyl)indol-3-yl]glyoxylamide derivatives **19** or **20** (0.5 mmol) in 10 mL of dry dichloromethane cooled at -10 °C were added dropwise 0.2 mL of BBr_3. The mixture was left under stir-ring for 30 min. at -10 °C, and subsequently at room temperature for 1h under nitrogen atmosphere (TLC analysis with appropriate eluent). Finally, the solution was cooled again, and was added 5 ml of methanol to hydrolyze the excess of BBr_3. The solvent was evaporated at reduced pressure, and the solid precipi-tate was washed several times with methanol. The residues obtained were purified by recrystallization from toluene (**35**) or by flash chromatography for compounds **36** (eluent system, petroleum ether/ethyl acetate in 5:5 ratios).

Yields, melting points, and spectral data of compounds **35-36** are listed in ***TABLE 2***.

General procedure for the synthesis of:

4-(3-dialkylaminoglyoxylylindol-2-yl)benzoic acid derivatives (**37-39**):

Lithium hydroxide monohydrate (0.3 mmol) was added to a suspension of methyl 4-(3-dialkylaminoglyoxylylindol-2-yl)benzoate derivatives **22-24** (0.5 mmol) in 20 mL of a MeOH/H_2O (3:1) solution. The mixture was stirred under reflux at 80 °C overnight (TLC analysis with appropriate eluent). Subsequently, the solid precipitate was eliminate through vacuum filtration, and the solution was acidified with HCl dil. 10% to pH 5. The acid precipitated in the solution was collected by filtration and generally did not needed any further purification.

Yields, melting points, and spectral data of compounds **37-39** are listed in ***TABLE 2***.

BIOCHEMICAL SECTION:

The binding assay is a biochemical method by which to identify the binding sites through the use of radioisotopes. It should make a distinction between the receptor and binding site: a receptor site is a competition site for the agonist and antagonist. The stimulus produced by the binding of the agonist to the receptor leads to a physiological response. On the contrary, a binding site is only an acceptor site to which it is not necessarily connected the transmission of a signal and then a cellular response. From an experimental point of view, the binding site is related to the receptor site when there is a correlation between the affinity of the ligand in vitro and in vivo pharmacological potency, tissue specificity, stereospecificity, saturability, reversibility and high affinity. The method of the radioactive binding

provides the incubation of a biological preparation, which contains the receptor with a radiolabelled ligand specific for that receptor, under conditions of time, temperature and pH sufficient to attain equilibrium. During the incubation time, a certain amount of ligand (**L**) with the receptor (**R**) forms the receptor-ligand complex (**RL**); the excess amount of free **L**, is separated from the **RL** by subsequent vacuum filtration. This procedure must be made quickly and with cold buffer so as to minimize the possibility of dissociation of the complex. The formation of the complex **RL** is a reversible reaction regulated by the law of mass action and characterized by constants of association (K_1) and dissociation (K_2):

$$L + R \underset{K_2}{\overset{K_1}{\rightleftharpoons}} RL$$

At the equilibrium, the rate of association and dissociation assume the same value, then:

$$\upsilon_a = \upsilon_d \longrightarrow K_1 \times [RL] \longrightarrow \frac{[RL]}{[L][R]} = \frac{K_1}{K_2}$$

$K_1 / K_2 = K_a$ association constant.

The total binding of the radioligand to the receptor (**LT**) is determined incubating the membranes with the radioligand, and is composed of specific binding (**SB**) and non-specific binding (**NB**) of the radioligand. The **NB** corresponds to the amount of radioligand which binds to non-specific structures not receptorial and is determined incubating the membranes with the radioligand, in the presence of saturating concentration of a ligand specific and selective for the same receptor site. In this way, competing with the radioligand, but being in a concentration greater, occupies

all the binding sites. The non-specific binding must be as low as possible (20-30% of total). Then the specific binding is calculated as the difference between total binding (measured in the absence of competitive agent) and represents 70-80% of total binding. Membranes containing the receptor of interest are incubated with a constant concentration of radioligand in the presence of increasing concentrations of competitor ligand. Incubating the membranes with the radioligand is possible to quantify the power of the ligand of interest. In terms of competitor the concentration of that effectively inhibits by 50% the specific binding of the radioligand (**IC_{50}**). The **IC_{50}** can be calculated through the analysis of non-linear regression. Using an appropriate table, the percentages of inhibition of radioligand binding of the are converted into probability of inhibition. The values obtained are indicated in the ordinate, while on the abscissa are reported the corresponding concentrations in logarithmic scale of the competitor.(***FIGURE(12)***)From the equation of the straight line is possible to obtain the value of **IC_{50}**.

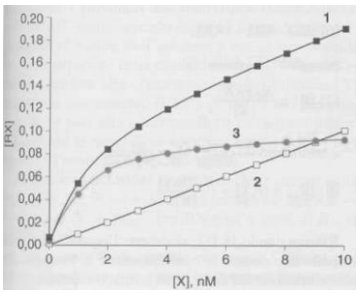

FIGURE(12): *Graph of the specific binding (circles curve), the nonspecific binding (empty squares straight line) and total (squares curve blacks).*

The **IC_{50}** determined in binding studies is transformed into inhibition constant **K_i** of the competitor, through the use of the equation of Cheng and Prusoff:

$$K_i = IC_{50} / (1 + [L] / K_d)$$

Where: K_i = inhibition constant of the competitor

K_d = dissociation constant of the radioligand

[L] = concentration of the radioligand

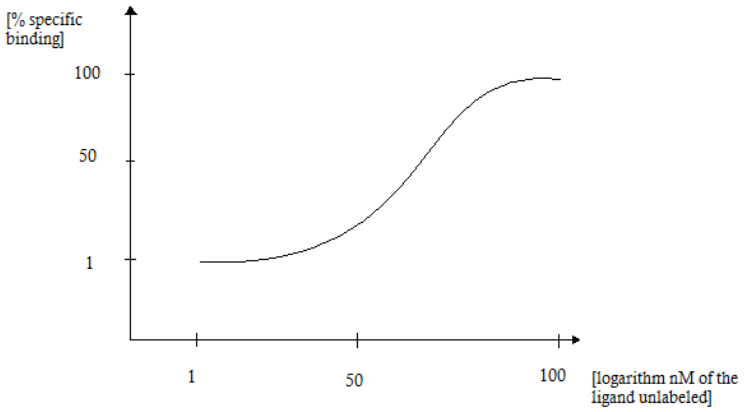

FIGURE(13): *example of curve placement.*

Specific binding, as a saturable phenomenon, increases until reaching a plateau (steady state). The nonspecific binding increases linearly as a function of ligand concentration. This is due to the fact that the non-specific binding is given by the interaction of the ligand with the receptor sites, or more simply by radioactivity absorbed by the filter. The measurement of residual radioactivity is performed by a scintillator in the liquid phase that provides the disintegrations per minute (***dpm***). From the value of ***dpm*** is possible to trace the μC_i present in the samples through the following relation:

1 μC_i = 2.220.000 ***dpm***

Finally, knowing the specific activity of the radioligand (**SA = μC$_i$ / mol**), is possible to determine the nanomoles of radioligand present as a complex ***LR*** to equilibrium (Bound = pmol (or fmol) / mg of protein). In this work, the studies about the affinity of TSPO ligands were performed using preparations of rat kidney membrane,as,and radioligand [^{3}H]PK11195.

✓ *MATERIALS AND METHODS:*

The preparation of the mitochondrial membranes of rat kidney was carried out as described by Campiani et al.(1996) and Trapani et al.(1997). The kidney was minced and suspended 1:10 in buffer 50 mM Tris-HCl, pH 7.4 (T50), 0:32 M sucrose containing, 1 mM EDTA and protease inhibitors (benzamidine 160 mg/ml, bacitracin 200 mg/ml, trypsin inhibitors 20 mg/ml). The obtained suspension was homogenized and then centrifuged at 600 x g for 10 minutes at a temperature of 4° C. The supernatant (**S1**) was again centrifuged at 10000 x g for 10 minutes at 4 ° C. The precipitate obtained from the latter centrifugation (**P2**) was resuspended in relation 1:20 with buffer T50 and recentrifuged at 10000 x g for 10 minutes at 4° C. By centrifugation was obtained a pellet (**P3**) containing the mitochondrial membranes that were stored at -20 ° C until the moment of their use.

✓ *DETERMINATION OF PROTEIN CONCENTRATION:*

To determine the protein content, present in a biological sample, was performed a proteic dosage that includes the use of radioactive commercial Biorad Protein Assay (Bradford method colorimeter). This assay employs the dye Coomassie

Brilliant Blue G-250, which changes color in response to bond with the amino acid residues of which mainly aromatic or basic. The assay was performed by adding aliquots of the membranes to 200 µl of reagent and the quantity of distilled water necessary to reach a coloring bluish, whose intensity is directly proportional to the concentration of proteins. ***TABLE 3***

	Buffer	**Membranes**	**Water MQ**	**Biorad**
B	20 µl	/	780 µl	200 µl
B'	20 µl	/	780 µl	200 µl
M	/	20 µl	780 µl	200 µl
M'	/	20 µl	780 µl	200 µl

TABLE 3: Preparation protein assay

It was then measured the absorbance in a spectrophotometer at a wavelength of 595 nm. From the absorbance value obtained was the concentration of protein present in the sample by reference to the calibration curve obtained using solutions of γ-globulin to increasing conncentrations (2.5 - 20 µg/mL). (***Figura (14)***)

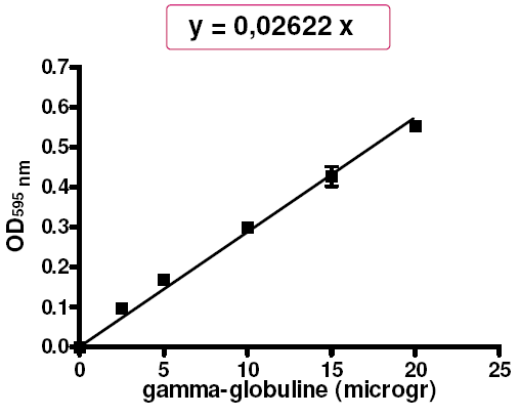

FIGURE(14): *Calibration curves Biorad Red*

✓ *DETERMINATION OF THE BINDING OF RADIOLIGAND TO THE TSPO IN PRESENCE OF NEW SYNTHESIZED COMPOUNDS:*

The method involves the incubation of aliquots of membranes containing approximately 15 μg of protein, with a constant concentration of radioligand ([^{3}H] PK 11195), 0.6 nM for 90 minutes at 4 ° C. The nonspecific binding is determined incubating an aliquot of membranes in the presence of PK11195 1 μM (not labeled), as an agent competitor. The new synthesis compounds were added to the incubation mixture at increasing concentrations (0.1 nM-10μM) after being dissolved in dimethyl sulfoxide (**DMSO**). After 90 minutes of incubation the samples were subjected to vacuum filtration on filters of glass wool Whatmann GF/C and performing two washes in a tube with 4 ml of cold 50 mM Tris buffer. Each filter is then inserted into a plastic vial with 4 ml of *Ultima Gold* ^{TM} scintillation liquid. The counts of the residual radioactivity on the filter is effected by a scintillator in the liquid phase (TRI-CARB 2800 TR). From the curve of competing ligand, which competes for binding to the receptor site, it is possible to determine the concentration of competitor which inhibits 50% of the specific binding of the radioligand (**IC_{50}**) and through the equation of Cheng-Prusoff (1973) is calculated the inhibition constant **K_i**. (an example of binding curve is reported in ***FIGURE(15).***

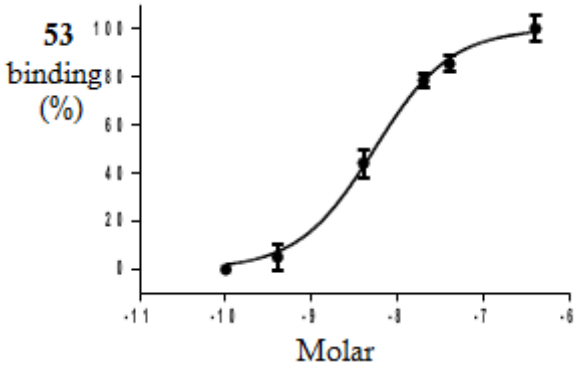

EC 50	5.339 e•0.09
Ki	3.820 e•0.09

FIGURE(15): *Graph example of binding of the compound* ***34****.*

In this work binding studies were performed to assess the activity of newly synthesized compounds for Translocator protein 18kDa. Has been verified that the structural changes designed on the pharmacophore model proposed by Dalpiaz (Dalpiaz et al.,1995) have really led to a lowering of the constant K_i. The K_i values were reported in ***TABLE 4***.

PROLIFERATION STUDIES:

On the basis of their structures and affinity costant values to TSPO, the compounds **21**, **22**, **30** and **31** were selected to perform proliferation studies in metabolic stress conditions like the ones exerted in nutrient deprivation (starvation). The condition of serum deprivation for proliferation assay is common used render the cells qluiescents and ti have more reliable results after cell stimulation. By the way, some cells are more susceptible towards low serum medium in that they go into spontaneus apoptosis. A human cell line derived from a glial lineage (U87MG) was used for these preliminar experiments. This cell line was provided by the National Institute for Research of Cancer (ICLC) in Genoa. These compounds were selected

on the basis of their affinity, evaluated in terms of K_i. They have substituents "Ar" with a good ratio hydrophilicity / lipophilicity, essential for interactions with binding site, and also have the right dimensions that allow them to fit perfectly in the pocket receptor. The compounds **21** and **22** carry, in position 2 of the indole, a *p*-OCH_3-C_6H_4. The compounds **30** and **31**, however, carry the thiophene. What distinguishes between them the two pairs of compounds are the substituents R_1 and R_2, which may be chains butyl or hexyl. This choice has been made to verify that the possible neuroprotective effect is due to the substituent in position 2 of the indole or to the length of the alkyl chains on the amide nitrogen, to increase of which has larger dimensions but also greater capacity for torsion of molecule.

- ✓ ***Thawing procedure***

The cells, stored in liquid nitrogen in criovials, have been quickly heated in the bath at 37° C and harvested. Following, pre-heated complete medium is added very slowly ,and the whole is then centrifuged at 100 xg for 5 minutes. The pellet obtained is then resuspended in an appropriate volume of heated complete medium. The suspension obtained is then transferred into a flask of 75 cm^2, already containing complete medium, so as to obtain total 10 ml and it was then maintained at 37° C in the incubator with a humidified atmosphere of 5% CO_2 and 95% of O_2.

- ✓ ***Conditions of cell culture:***

The cells were plated and maintained in the appropriate sterile complete culture medium consisting of:

- RPMI-1640 (1:1);
- 10% of fetal bovine serum (FBS);
- Pen-Strep 100 U/mL (antibiotic which prevents the proliferation of bacteria.)
- L-glutamine 2 mM;
- 1% non-essential amino acids;

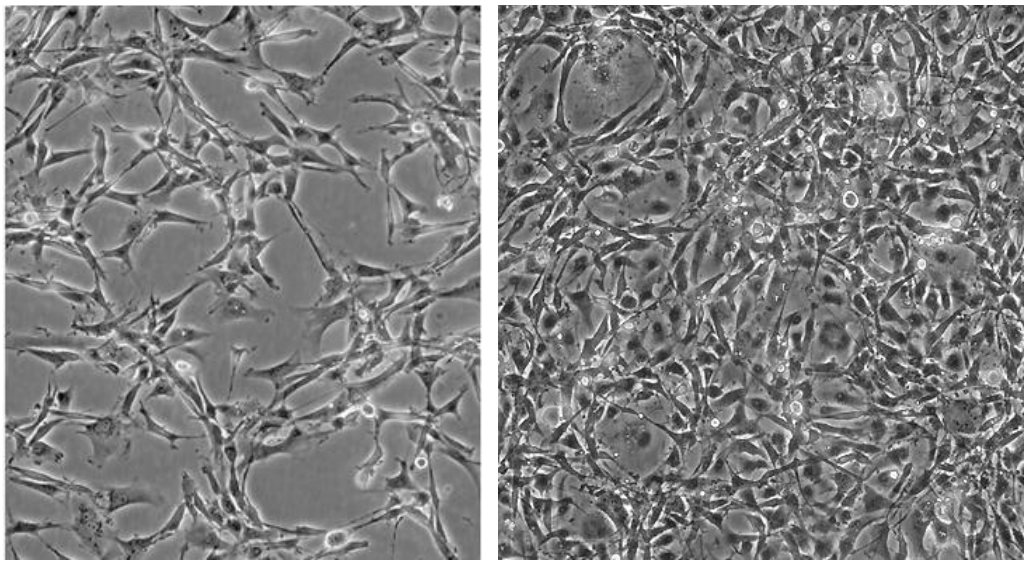

FIGURE(16): *U87MG cells. Low density (on the left) and high density (on the right).*

✓ *Splitting technique:*

This technique, also called trypsinization, allows the detachment of eukaryotic cells adherent to a solid substrate. The trypsinization is done through the use of a solution containing the enzyme trypsin (a protease that breaks down the proteins in the joints, creating interconnections between cells), and EDTA which at high concentrations chelates Ca^{2+}, essential for cell adhesion. The experimental procedure involves the use of the culture medium, the solution of Trypsin-EDTA

and saline solution, all previously heated to 37° C. The culture medium is aspirated from the flask using a glass Pasteur connected to a vacuum pump, then a washing is carried with the saline and aspirating means. Subsequently add a volume (related to the number of cells present in the flask) of the solution Trypsin-EDTA and left in incubation at 37 ° C for a few minutes. If, observing with an optical microscope, the cells contained in the flask are detached, there are introduced 3-4 ml of culture medium that neutralizes the trypsin. Then is withdrawn the suspension by washing well the surfaces of the flask with the medium and the whole is transferred in a 15 ml falcon previously prepared with 2 ml of culture medium. The cell suspension is then centrifuged to 300 rpm for 5 minutes at r.t. The supernatant is aspirated carefully and the pellet obtained is resuspended in a suitable volume of culture medium by homogenization accurate.

- ✓ ***Cell seeding:***

In a 96-multiwell were seeded at a density ~8000 cells / well. Cells were maintained at 37° C in the incubator with a humidified atmosphere of 5% CO_2 for 24h.The day after, cells were added with compounds in serum deprivation using 1% FBS. PK11195 was used as positive controls. Indeed it was been reported thet PK11195 increased the growth rate of C6 glioma cells by 20-30% in the nanomolar range in serum free medium. [37] The control cells were treated with veihcle alone the compounds. The cells were treated in duplicate with the compounds **21**, **22**, **30** and **31** at three different concentrations (10 nM, 100nM and 1 μM). After 48 h the MTS assay and crystal violet staining were performed .

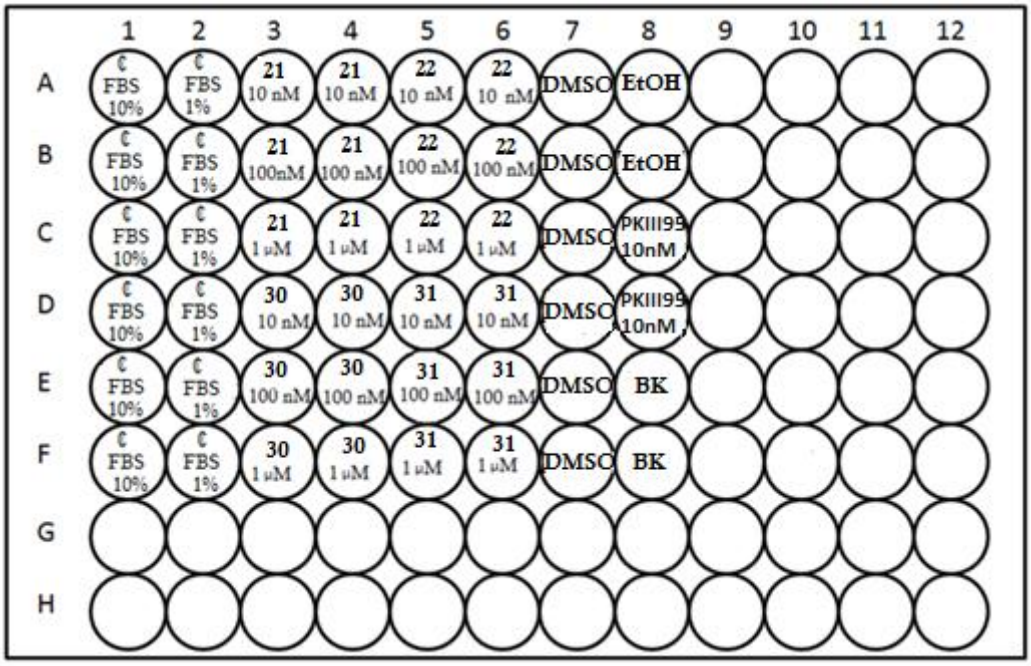

FIGURE(17): *In a 96-multiwell were seeded ~8000 cells / well. 10 nM PK11195 was used as positive controls. The untreated cells were cultured with complete medium and with deprivation of 1% FBS. The cells were treated in duplicate with the compounds* ***21****,* ***22****,* ***30*** *and* ***31*** *at three different concentrations (10 nM, 100 nM and 1* µ*M).*

- ✓ ***MTS assay:***

MTS is a colorimetric method that allows to determine the number of viable cells in a proliferation or cytotoxicity assay. It is based on use of the reagent liquid tetrazolium (MTS) that within the cells is reduced to formazan (composed of bluish) by mitochondrial enzyme succinate dehydrogenase. Cell viability was determined spectrophotometrically by measuring the conversion of the MTS substrate to the formazon product which is directly proportional to the number of viable cells. The reaction can take place only in metabolically active cells and the value of optical density, obtained by spectrophotometric reading, can be correlated to the quantity of viable cells present.

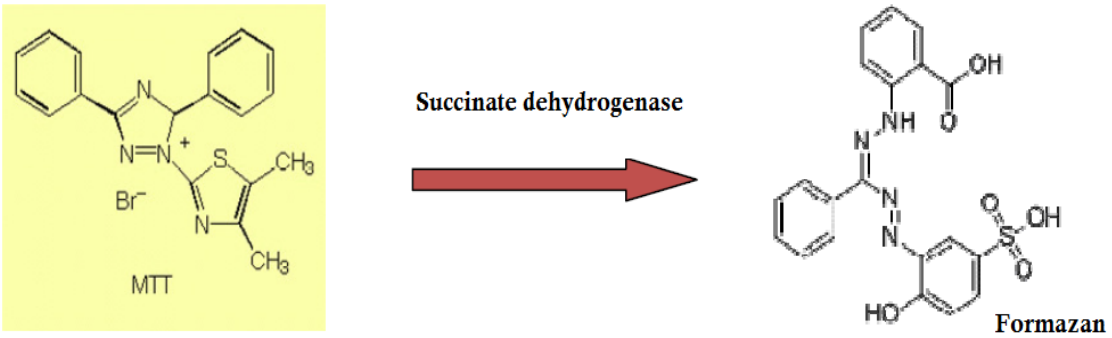

FIGURE(18): *Reaction scheme leading to the formazan.*

- ✓ ***Crystal violet:***

Crystal violet (**CV**) is a triphenylmethane dye (4-[(4-dimethylaminophenyl)-phenyl-methyl]-*N*,*N*-dimethyl-aniline) also known as *Gentian violet*. The most commonly used application for this dye is as the primary microbiological stain in the Gram-staining procedure used to The CV assay was initially used to quantify the cell number in monolayer cultures as a function of the absorbance of the dye taken up by the cells differentiate bacteria. However, this method is now being used, after some modification, for a wide number of applications including determination of cytotoxicity or cell death produced by chemicals, drugs, or toxins from pathogens , to determine cell viability or to determine cell proliferation under different testing conditions. CV is a simple assay that is useful for obtaining quantitative information about the relative density of cells adhering to multi-well cluster dishes. However, note that this dye stains DNA and the color of the dye depends upon the pH of the solution. Upon solubilization, the amount of dye taken-up by the

monolayer and the intensity of the color produced are proportional to cell number.[36]

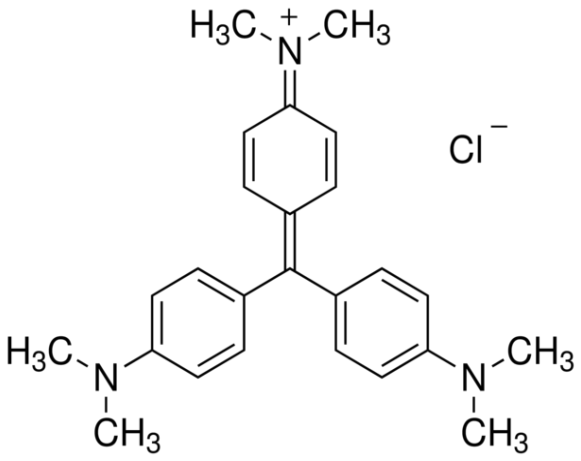

FIGURE(19): *Crystal violet solution.*

RESULTS AND DISCUSSION:

In this study, a series of novel *N*,*N*-dialkyl-2-arylindol-3-ylglyoxylamide TSPO ligands was designed, synthesized and tested for their affinity toward TSPO and for their ability to influence cell growth in vitro.

TABLE 4: Ki values for the compounds tested for displacement of ^{3}HPK 11195 in membranes of rat kidney.

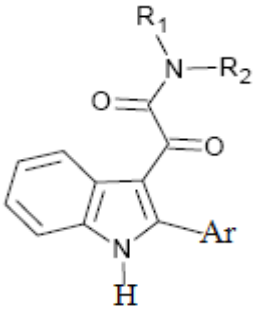

n	R_1=R_2	Ar	Ki (nM) [a]
Id	$(CH_2)_2CH_3$	Ph	12,2±1,0
Ie	$(CH_2)_3CH_3$	Ph	7,5±0,7
If	$(CH_2)_4CH_3$	Ph	16,0±0,2
Ig	$(CH_2)_5CH_3$	Ph	1,4±0,2
20	$(CH_2)_2CH_3$	*p*-OCH_3-C_6H_4	5,82±0,5
21	$(CH_2)_3CH_3$	*p*-OCH_3-C_6H_4	20,34±2
22	$(CH_2)_5CH_3$	*p*-OCH_3-C_6H_4	4,037±0,4
23	$(CH_2)_2CH_3$	*p*-$COOCH_3$-C_6H_4	3,101±0,3
24	$(CH_2)_3CH_3$	*p*-$COOCH_3$-C_6H_4	2,735±0,3
25	$(CH_2)_5CH_3$	*p*-$COOCH_3$-C_6H_4	3,275±0,3
29	$(CH_2)_2CH_3$	thiophene	1,234±0,12
30	$(CH_2)_3CH_3$	thiophene	2,829±0,3
31	$(CH_2)_5CH_3$	thiophene	0,8903±0,1

32	$(CH_2)_2CH_3$	*p*-NH_2-C_6H_4	44,4±0,5
33	$(CH_2)_3CH_3$	*p*-NH_2-C_6H_4	132,8±13,3
34	$(CH_2)_5CH_3$	*p*-NH_2-C_6H_4	3,820±0,4
35	$(CH_2)_2CH_3$	*p*-OH-C_6H_4	16,3±1
36	$(CH_2)_3CH_3$	*p*-OH-C_6H_4	25,65±2,6
37	$(CH_2)_2CH_3$	*p*-COOH-C_6H_4	343,0±10
38	$(CH_2)_3CH_3$	*p*-COOH-C_6H_4	406,4±41
39	$(CH_2)_5CH_3$	*p*-COOH-C_6H_4	183,9±20

[a] K_i values are expressed as mean ± SEM of three determinations.

At first, the analysis of the binding affinity of all the novel compounds **20-25**, **29-39** for TSPO was performed in order to select the ligands with the highest affinity and evaluate their potential as neuroprotective agents. The binding affinity to TSPO of the novel compounds was determined in competition binding studies using the radioactive ligand [^{3}H]PK11195 in homogenates of rat kidney membranes. From the analysis of the competition curves for each ligand, the value of K_i, i.e. the concentration of the compound that inhibits the binding of [^{3}H]PK11195 to the mitochondrial membrane of rat kidney of 50%, is derived. In ***TABLE 4*** the affinity data of the newly synthesized products **20-25**, **29-39** are reported, together with those of derivatives **Id**, **Ie**, and **Ig** for comparison purpose. It should be noted that, in general, we have obtained highly affine TSPO ligands, as most of the novel compounds show K_i values in the low nanomolar range. The best performant modification at 2-position of the indole scaffold results to be the insertion of a thienyl nucleus, showing compounds **29**, **30** and **31** the highest affinity of the whole series with Ki values of 1.234 nM, 2.829 nM, and 0.8903 nM. In addition, the 2-thienyl derivatives **29**, **30** and **31** present a gain in affinity with respect to their

corresponding 2-phenyl-substituted counterparts **Id**, **Ie**, and **Ig**, of about 10-, 3-, and 2-fold, respectively. These data could be rationalized by hypothesizing that the thiophene ring, due to its lipophilicity and limited steric-demanding dimensions, permits an efficacious lipophilic interaction at the level of the L_1 pocket.

The insertion of different substituents at the para position of the 2-phenyl ring (derivatives **20-25**, **32-39**) produces effects on TSPO affinity that depend both on the hydrophilic/lipophilic characteristics of the group and the length of the alkyl chains bounded to the glyoxylamide nitrogen, sometimes in an interdependent way. A number of main structure-affinity relationships could be drawn.

Compounds bearing an highly hydrophilic 4'-substituents, such as NH_2, OH, and COOH show a general decrease in affinity with respect to their 4'-unsubstituted analogs, with few exceptions: the amino and the hydroxy groups are tolerated in the presence of *N*,*N*-dihexyl and *N*,*N*-dipropyl side chains, respectively (**34** K_i 3.820 nM vs **Ig** K_i 1.4 nM, and **35** K_i 16.3 nM vs **1d** K_i 12.2 nM).

Conversely, insertion of a 4'-lipohilic group such as OCH_3, $COOCH_3$, yields compounds **20-25** with comparable or higher TSPO affinity than the unsubstituted counterparts, with the only exception of compound **21**.

Taken together all these data seem to indicate that the nature of the L_1 pocket is mostly lipophilic, as polar substituents, differently from the lipophilic ones, are not able to engage efficacious interactions with it.

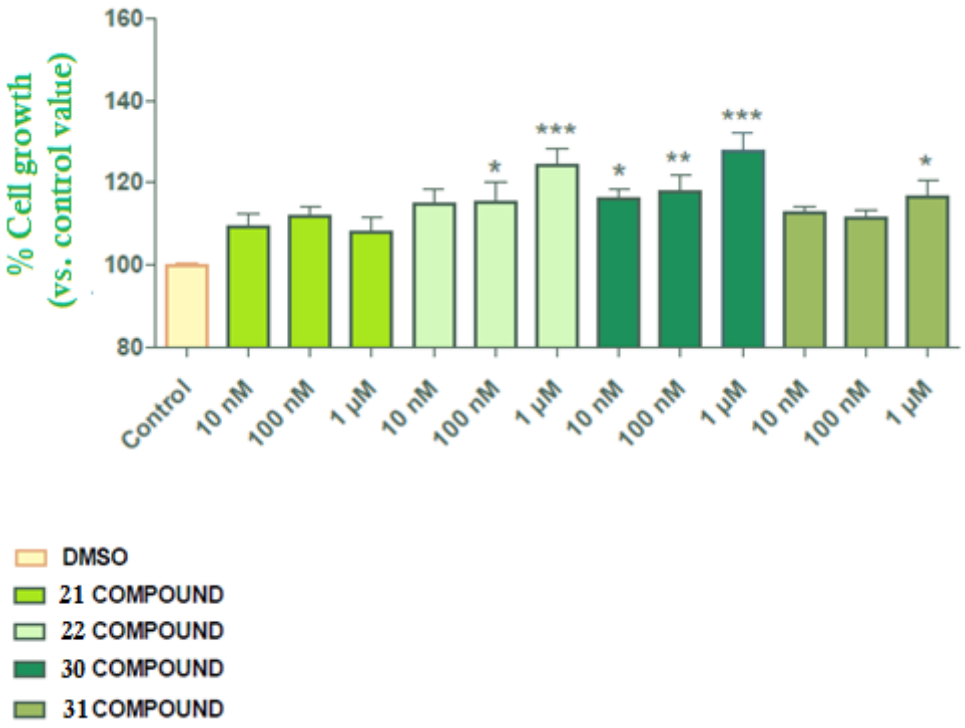

FIGURE(20): *Effect of novel TSPO ligands on cell growth. U87MG cells.Results are expressed as a percentage of viable cells observed after treatment with ligands vs. untreated control cells (100%) and shown as mean SEM derived from least three separate experiments done in duplicate. P < 0:05 with respect to control, one-way ANOVA (Newman–Keuls test).*

In light on SAR analysis, the compounds **21**, **22**, **30** and **31** were selected to perform proliferation studies in starvation. Firstly, it has been observed a reduction of the not treated cell number cultured in 1% FBS in respect to complete medium (above 30%) (data not shown), indicating a reduction in growth rate due to a cell quiescient state or a spontaneous apoptosis. The data obtained with the novel TSPO ligands suggest that in each sample of cells, treated with the nanomolar concentrations of compounds, there was an increase in growth rate in respect to the control with DMSO. However, compound **21** has proved only a trend toward increase (not statistically significant). For the other compounds, the statistical analysis showed a significant concentration-dependent increase the cell growth.

Particularly effective is compound **30** which, at increasing concentration, showed increasing neuroprotective activities (***FIGURE(20)***). The classical TSPO ligand PK11195 elicited a 30% increase in cell number at 10 nM, according to preavious literature.[37] These findings suggest that TSPO may be involved in the control of cell growth: a possible mecchanism eliciting such effect is the production of steroids. Indeed, it is well-known that TSPO-ligands interaction led to increase in production of steroids, that in turn exert benefical and survival effects on cell metabolism. If such preliminary results are confirmed even in a cellular model of primary neurons or in a neurodegenerative cell model, these compounds may be used as versatile scaffold for the design of novel neuroprotective agents.

REFERENCES:

[1] Shorter E (**2005**). "Benzodiazepines". A Historical Dictionary of Psychiatry. Oxford University Press. pp. 41–2.

[2] Costa, E.; Guidotti; A. Molecular mechanisms in the receptor action of benzodiazepines. Annu. Rev. Pharmacol. Toxicol. **1979**, 19. 531-545.

[3] Chebib, M.; Johnson; G. GABA-activated ligand gated ion channels: medicinal chemistry and molecular biology. J. Med. Chem. **2000**, 43, 1427-1447.

[4] Braestrup, C.; Squires; R. Specific benzodiazepine receptors in rat brain characterized by high affinity [1H]diazepam binding. Proc. Natl. Acad. Sci. U.S.A. **1977**, 74, 3805-3809.

[5] Taliani, S.; Pugliesi, I.; Da Settimo, F.; Structural requirements to obtain highly po-tent and selective 18 kDa translocator protein (TSPO) ligands. Curr. Top. Med. Chem. **2011**, 11, 860-886.

[6] Papadopoulos, V.; Baraldi, M.; Guilarte, T. R.; Knudsen, T. B.; Lacapère, J.; Lindemann, P.; Norenberg, M. D.; Nutt, D.; Weizman, A.; Zhang, M. R.; Gavish, M.; Translocator protein (18 kDa): new nomenclature for the peripheral-type benzodiaze-pine receptor based on its structure and molecular function. Trends Pharmacol. Sci. **2006**, 27, 402-409.

[7] Scarf, A. M.; Ittner, L. M.; Kassiou, M; The translocator protein (18 kDa): central nervous system disease and drug design. J. Med. Chem. **2009**, 52, 581-592.

[8] McEnery, M. W.; Snowman, A. M.; Trifiletti, R. R.; Snyder, S. H.; Isolation of the mi-tochondrial benzodiazepine receptor: association with the voltage-dependent anion channel and the adenine nucleotide carrier. Proc. Natl. Acad. Sci. USA **1992**, 89, 3170-3174.

[9] Blahos II, J.; Whalin, M. E.; Krueger, K. E.; Identification and purification of a 10-kilodalton protein associated with mitochondrial benzodiazepine receptors. J. Biol. Chem. **1995**, 270, 20285-20291.

[10] Galiègue, S.; Jbilo, O.; Combes, T.; Bribes, E.; Carayon, P.; Le Fur, G.; Casallas, P.; Cloning and Characterization of PRAX-1. J. Biol. Chem. **1999**, 274, 2938-295.

[11] Papadopoulos, V.; Lecanu, R.; Brown, R. C.; Han, Z.; Yao, Z. X.; Peripheral-type benzodiazepine receptor in neurosteroid biosynthesis neuropathology and neurological disorders. Neuroscience. **2006**, 138, 749-756.

[12] Hauet, T.; Yao, Z. X.; Bose, H. S.; Wall, C. T:; Han, Z.; Li, W.; Hales, D. B.; Miller, W. L.; Culty, M.; Papadopoulos, V.; Peripheral-type benzodiazepine receptor-mediated action of steroidogenic acute regulatory protein on cholesterol entry into Leydig cell mitochondria. Mol. Endocrinol. **2005**, 19, 540-554.

[13] Li, H.; Degenhardt, B.; Tobin, D.; Yao, Z. X.; Tasken, K.; Papadopoulos, V.; Identification, localization, and function in steroidogenesis of PAP7: a peripheral-type benzodiazepine receptor- and PKA (RIα)-associated protein. Mol. Endocrinol. **2001**, 15, 2211-2228.

[14] Beurdeley-Thomas, A.; Miccoli, L.; Oudard, S:; Dutrillaux, B.; Poupon, M. F.; The peripheral benzodiazepine receptors: a review. J. Neurooncol. **2000**, 46, 45-56.

[15] Gavish, M.; Bachman, I.; Shoukrun, R:; Katz, Y:; Veenman, L.; Weisimger, G.; Weiz-man, A.; Enigma of the peripheral benzodiazepine receptor. Pharmacol. Rev. **1999**, 51, 629-650.

[16] Da Settimo, F.; Simorini, F.; Taliani, S.; La Motta, C.; Marini, A. M.; Salerno, S.; Bellandi, M.; Novellino, E.; Greco, G.; Cosimelli, B.; Da Pozzo, E.; Costa, B.; Simola, N.; Morelli, M.; Martini, C.; Anxiolytic-like effects of N,N-dialkyl-2-phenyliindol-3ylglyoxylamides by modulation of translocator protein promoting neurosteroid biosynthesis. J. Med. Chem., **2008**, 51, 5798-5806.

[17] Costa, B; Da Pozzo, E.; Chelli, B.; Simola, N.; Morelli, M.; Luisi, M.; Maccheroni, M.; Taliani, S.; Simorini, F.; Da Settimo, F.; Martini, C.; Anxiolytic properties of a 2-phenylindolglyoxylamide TSPO ligand: stimulation of in vitro neurosteroid production affecting $GABA_A$ receptor activity. Psychoneuroendocrinology, **2011**, 36, 463-472.

[18] Casellas P.; Galiegue, S.; Basile, A. S.; Peripheral benzodiazepine receptors and mitochondrial function. Neurochem. Int. **2002**, 40, 475-486

[19] Azarashvili, T.; Grachev, D.; Krestinina, O.; Evtodienko, Y.; Yurkov, I.; Papadopoulos, V:; Reiser, G:; The peripheral-type benzodiazepine receptor is involved in control of Ca2+-induced permeability transition pore opening in rat brain mitochondria. Cell Calcium, **2007**, 42, 27-39.

[20] Galiegue, S.; Tinel, N.; Casellas, P.; The peripheral benzodiazepine receptor: a promising therapeutic drug target. Curr. Med. Chem., **2003**, 10, 1563-1572.

[21] Cagnin A., KAssiou M., Meikle S.R., Banati R.B. Positron emission tomography imaging of neuroinflammation. Neurotherapeutics. **2007** Jul; 4(3):443-52.

[22] Chelli, B.; Salvetti, A.; Da Pozzo, E.; Rechichi, M.; Spinetti, F.; Rossi, L.; Costa, B.; Lena, A.; Rainaldi, G.; Scatena, F.; Vanacore, V.; Gremigni, V.; Martini, C.; PK 11195 differentially affects cell survival in human wild-type and 18 kDa Translocator Protein-silenced ADF astrocytoma cells. J. Cell. Biochem. **2008**, 105, 712-723.

[23] Pike, V.W.; Taliani, S.; Lohith, T.G.; Owen, D.R.J.; Pugliesi, I.; Da Pozzo, E.; Hong, J.; Zoghbi, S.S.; Gunn, R.N.; Parker, C.A.; Rabiner, E.A.; Fujita, M.; Innis, R.B.; Martini, C.; Da Settimo, F.; Evaluation of novel N1-methyl-2-phenylindol-3-ylglyoxylamides as a new chemotype of 18 kDa Translocator Protein-selective ligand suitable for the development of Positron Emission Tomography radioligands. J. Med. Chem., **2011**, 54, 366-373.

[24] Primofiore, G.; Da Settimo, F.; Taliani, S.; Simorini, F.; Patrizi, M.P.; Novellino, E.; Greco, G.; Abignente, E.; Costa, B.; Chelli, B.; Martini, C.; *N*,*N*-dialkyl-2-phenylindol-3-ylglyoxylamides. A new class of potent and selective ligands at the peripheral benzodiazepine receptor. J. Med. Chem., **2004**, 47, 1852-1855.

[25] Wadsak, W.; Mitterhauser, M.; Basics and principles of radiopharmaceuticals for PET/CT. Eur. J. Radiol., **2010**, 73, 461-469.

[26] Taliani, S.; Da Pozzo, E.; Bellandi, M.; Bendinelli, S.; Pugliesi, I.; Simorini, F.; La Motta, C.; Salerno, S.; Marini, A.M.; Da Settimo, F.; Cosimelli, B.; Greco, G.; Novellino, E.; Martini, C.; Novel irreversible fluorescent probes targeting the 18 kDa Translocator Protein: synthesis and biological characterization. J. Med. Chem., **2010**, 53, 4085-4093.

[27] Basu, S.; Kwee, T.C.; Surti, S.; Akin, E.A.; Yoo, D.; Alavi, A.; Fundamentals of PET and PET/CT imaging. Ann. N. Y. Acad. Sci., **2011**, 1228, 1-18.

[28] Doorduin, J.; de Vries, E.F.J.; Dierckx, R.A.; Klein, H.C.; PET imaging of the peripheral benzodiazepine receptor: monitoring disease progress and therapy response in neurodegenerative disorders. Curr. Pharm. Design., **2008**, 14, 3297-3315.

[29] Matarrese, M.; Moresco, R.M.; Cappelli, A.; Anzini, M.; Vomero, S.; Simonelli, P.; Verza, E.; Magni, F.; Sudati, F.; Soloviev, D:; Todde, S.; Carpinelli, A.; Kienle, M.G.; Fazio, F.; Labeling and evaluation of N-[^{11}C]methylated quinoline-2-carboxamides as potential radioligands for visualization of peripheral benzodiazepine receptors. J. Med. Chem., **2001**, 44, 579-585.

[30] Zhang, M.R.; Ogawa, M.; Maeda, J.; Ito, T.; Noguchi, J.; Kumata, K.; Okauchi, T.; Su-hara, T.; Suzuki, K.;[2-^{11}C]isopropyl-, [1-^{11}C]ethyl-, [^{11}C]methyl-labeled phenoxyphenyl acetamide derivatives as Positron Emission Tomography ligands for the peripheral benzodiazepine receptor: radiosynthesis, uptake, and in vivo binding in brain. J. Med. Chem., **2006**, 49, 2735-2742.

[31] Doorduin, J.; Klein, H.C.; Dierckx, R.A.; James, M.; Kassiou, M.; de Vries, E.F.J.; [^{11}C]-DPA-713 and [^{18}F]-DPA-714 as new PET tracers for TSPO: a comparison with [^{11}C]-(R)-PK11195 in a rat model of Herpes Encephalitis. Mol. Imaging. Biol., **2009**, 11(6), 386-398.

[32] Taliani, S.; Simorini, F.; Sergianni, V.; La Motta, C.; Da Settimo, F.; Cosimelli, B.; Abignente, E.; Greco, G.; Novellino, E.; Rossi, L.; Gremigni, V.; Spinetti, F.; Chelli, B.; Martini, C. New fluorescent 2-phenylindolglyoxylamide derivatives as probes targeting the peripheral-type benzodiazepine receptor: design, synthesis, and biological evaluation. J. Med. Chem. **2007**, 50, 404–407.

[33] Hammond, M.L.; Zambias, R.A.; Chang, M.N.; Jensen, N.P.; McDonald, J.; Thomp-son, K.; Boulton, D.A.; Kopka, I.E.; Hand, K.M.; Opas, E.E. et al.; Antioxidant-based
inhibitors of leukotriene biosynthesis. The discovery of 6-[1-[2-(hydroxymethyl)phenyl]-1-propen-3-yl]-2,3-dihydro-5-benzofuranol, a potent topical antiinflammatory agent. J. Med. Chem., **1990**, 33, 908-918.

[34] Veenman, L.; Shandalov, Y.; Gavish, M.; VDAC activation by the 18 kDA translocator protein (TSPO), implications for apoptosis. J. Bioenerg. Biomembr., **2008**, 40, 199-205.

[35] Corey, E.J.; Székely, I.; Shiner, C.S.; Synthesis of 6,9a-oxido-11a, 15a-dihydroxy-prosta-(E)5, (E)13-dienoic acid, an isomer of PGI2 (vane's PGX). Tetrahedron Lett., **1977**, 18, 3529-3532.

[36] Elisa Vega-Avila and Michael K. Pugsley; An Overview of Colorimetric Assay Methods Used to Assess Survival or Proliferation of Mammalian Cells. Proc. West. Pharmacol. Soc. 54: 10-14, **2011**.

[37] Ikezaki K. and Black K.L. Stimulation of cells growth and DNA synthesis by peripheral Benzodiazepine. Cancer letters v. 49 (**1990**) pp. 115-120.

REFERENCES OF THE FIGURES:

Figure (1): Scarf, A. M.; Ittner, L. M.; Kassiou, M; The translocator protein (18 kDa): central nervous system disease and drug design. J. Med. Chem. **2009**, 52, 581-592.

Figure (2): McEnery, M. W.; Snowman, A. M.; Trifiletti, R. R.; Snyder, S. H.; Isolation of the mitochondrial benzodiazepine receptor: association with the voltage-dependent anion channel and the adenine nucleotide carrier. Proc. Natl. Acad. Sci. USA **1992**, 89, 3170-3174.

Figure (3): Sylvaine Galiègue, Omar Jbilo, Thèrèse Combes, Estelle Bribes, Pierre Carayon,Gèrard Le Fur§, and Pierre Casellas; Cloning and Characterization of PRAX-1:

A new protein that specifically interacts with the peripheral benzodiazepine receptor. The journal of biological chemistry. USA **1998,** 2945.

Figure (4): Thorsell, A.G., Lee, W.H., Persson, C., Siponen, M.I., Nilsson, M., Busam, R.D., Kotenyova, T., Schuler, H., Lehtio, L.; Comparative structural analysis of lipid binding START domains. (**2011**) Plos One 6: e19521-e19521.

Figure (5): Hua Li, BAbett Degenhardt, Derek Tobin, Zhixing Yao, Kjetil Tasken and VAssilios Papadopoulos; Identification, Localization, and Function in Steroidogenesis of PAP7: A Peripheral-Type Benzodiazepine Receptor- and PKA (RIα)-Associated Protein. (**2001**) Division of Hormone Research (H.L., B.D., Z.-X.Y., V.P.), Departments of Cell Biology, Pharmacology, and Neuroscience, Georgetown University School of Medicine, Washington, DC 20007; and Institute of Medical Biochemistry (D.T., K.T.), University of Oslo, N-0317 Oslo, Norway.

Figure (6): Papadopoulos, V.; Baraldi, M.; Guilarte, T. R.; Knudsen, T. B.; Lacapère, J.; Lindemann, P.; Norenberg, M. D.; Nutt, D.; Weizman, A.; Zhang, M. R.; Gavish, M.; Translocator protein (18 kDa): new nomenclature for the peripheral-type benzodiaze-pine receptor based on its structure and molecular function. Trends Pharmacol. Sci. **2006**, 27, 402-409.

Figure (7): Scarf, A. M.; Ittner, L. M.; Kassiou, M; The translocator protein (18 kDa): central nervous system disease and drug design. J. Med. Chem. **2009**, 52, 581-592.

Figure (8): Da Settimo, F.; Simorini, F.; Taliani, S.; La Motta, C.; Marini, A. M.; Salerno, S.; Bellandi, M.; Novellino, E.; Greco, G.; Cosimelli, B.; Da Pozzo, E.; Costa, B.; Simola, N.; Morelli, M.; Martini, C.; Anxiolytic-like effects of N,N-dialkyl-2-phenyliindol-3ylglyoxylamides by modulation of translocator protein promoting neurosteroid biosynthesis. J. Med. Chem., **2008**, 51, 5798-5806.

Figure (16): www.lgcstandards-atcc.org

Figure (19): www.sigmaaldrich.com